A Variational Calculation of the Trapping Current in a Thermal Barrier

X.Z. Li

January 1984

UWFDM-564

Ph.D. thesis.

FUSION TECHNOLOGY INSTITUTE

UNIVERSITY OF WISCONSIN

MADISON WISCONSIN

A Variational Calculation of the Trapping Current in a Thermal Barrier

X.Z. Li

Fusion Technology Institute
University of Wisconsin
1500 Engineering Drive
Madison, WI 53706

http://fti.neep.wisc.edu

January 1984

UWFDM-564

Ph.D. thesis.

A VARIATIONAL CALCULATION OF THE TRAPPING CURRENT IN A THERMAL BARRIER

by

XING ZHONG LI

A thesis submitted in partial fulfillment of the
requirements for the degree of

Doctor of Philosophy

NUCLEAR ENGINEERING

at the

University of Wisconsin-Madison

1983

A VARIATIONAL CALCULATION OF THE TRAPPING CURRENT

IN A THERMAL BARRIER

Xing Zhong Li

Under the supervision of Professor Gilbert A. Emmert

Although the ion distribution function in a thermal barrier is far from Maxwellian, the Fokker-Planck equation has been linearized and consequently a variational functional, which has the physical meaning of the trapping current, has been found. The variational method makes it possible to maintain the real shape and value of the boundary condition, and to retain the energy diffusion term in the collision operator. In order to solve this variational problem, a special trial function is proposed which uses only one variational parameter for an adequate description. We obtain an analytical expression, valid for the barrier mirror ratio from 2 to 20, for the pumping factor, g_b, or the trapping current J_t. Computer evaluation of the analytical expression is faster than the numerical Fokker-Planck code by a factor of at least 10^4. The comparison with Futch and LoDestro's numerical Fokker-Planck code results confirms our model. This variational method combined with the contour method to specify the trial function may be applicable in other problems.

APPROVED:

12/19/83

Date

Professor Gilbert A. Emmert
Department of Nuclear Engineering

ACKNOWLEDGMENTS

Many thanks go to Professor Gilbert A. Emmert for his inspiration and support during the course of this research. I am grateful to him for his friendly advice and the sometimes exciting discussions. This thesis is a part of the harvest resulting from my visit to the University of Wisconsin, which was initiated by Chancellor Shain. His enthusiasm has created a fruitful exchange program. Professor Max W. Carbon's quick response made it possible for me to be the first visitor from the People's Republic of China to the Nuclear Engineering Department in Madison. The Fusion Engineering Program headed by Professor Gerald L. Kulcinski provided me a productive and hospitable environment. I was lucky to arrive in Madison at the same time that Professor James D. Callen joined the UW faculty. His enlightening lectures and his plasma theory aficionados group are memorable. Many thanks for his continuous interest in my research. I would like to extend my heartfelt thanks to all the professors, scientists and staff in the Nuclear Engineering, Physics, and Electrical and Computer Engineering Departments for their friendship and help. Also, the opportunities to meet the scientists at Livermore and Princeton, at MIT, UC-Berkeley and UCLA, at RPI and the University of Iowa have been helpful. In particular, the visit to SAI Boulder Colorado opened a channel to Dr. Peter Catto, to whom I am grateful for his sincere and valuable help.

Special thanks go to Miss Beth Brown for her typing of this thesis. Her active help always improves the appearance of my manuscripts.

According to Chinese tradition, whoever drinks the water, always remembers the man who dug the well. Professor Robert Conn was my original sponsor who received me shortly before his leaving for UCLA.

Finally, it is my pleasure to thank Kernforschungszentrum Karlsruhe in the Federal Republic of Germany for their support. I hold my friendships with the scientists at KfK in very high regard.

DEDICATION

To My Motherland and the Cause of International Scientific Exchange.

Table of Contents

LIST OF FIGURES

1. INTRODUCTION

1.1 Motivation for the Study

Since the tandem mirror concept was first experimentally verified, the endloss problem in an open-ended configuration has been alleviated. The basic difference between open-ended and closed-ended systems is no longer the endloss, but the distribution function in velocity space. In an open-ended system, the distribution function of the plasma is in a non-equilibrium state, and thermal relaxation processes are the major concern.

Tracing the evolution of the tandem mirror configuration, we find that more and more cells are being added. After the end plug was first added (1976 [1]), the thermal barrier was invented (1978 [2]); this is a section between the central cell and end plug to provide thermal isolation of plug electrons from central cell electrons. Soon thereafter, an A-cell and other end-cell ideas appeared. The TARA device utilizes an axial-cell in conjunction with an anchor; some MFTF-B and MARS conceptual design configurations have also included an axicell. Regardless of the functions of these various cells, they are characterized by different densities and temperatures, and by different magnetic fields and electrostatic potentials. When these plasmas with different densities and temperatures interact with each other, various relaxation processes occur. In general, they are characterized by three collisional time scales: the ion-electron equilibration time, t_{eq}; the ion-ion scattering time, t_{ii};

the electron-electron scattering time, t_{ee}. Except for t_{eq}, the time scales are shorter than the confinement time scale of the plasma in a reactor. So, if there is no external power supply to maintain these different cells, the plasmas will decay. The power necessary to sustain the various cells is directly related to these relaxation processes, and the Q-value of a reactor is optimized when this power is reduced. Among these three time scales, t_{ee} is the shortest. If we use only the heating mechanism (such as ECRH, etc.) to maintain the cells at different electron temperature, we cannot afford the large input power required. Generally, one attempts to replace the t_{ee}-scale process by a t_{ii}-scale process. Then, the external power is used to support these t_{ii}-scale processes. Neutral beam injection, ICRH, etc. are examples. Since the t_{ii}-scale is longer than the t_{ee}-scale, the necessary power is reduced by a factor of (t_{ee}/t_{ii}) and becomes affordable. However, considering that the confinement time of the plasma in a tandem mirror is the same order or one order greater than t_{ii}, we are very concerned with these t_{ii}-scale processes. Since we often depend on the volume ratio of these different cells to reduce the power ratio of the external power supply to the fusion reaction power, the size of the reactor is dependent on our knowledge about these t_{ii}-scale processes.

These relaxation processes may be described by the evolution of the distribution function in velocity space with a separatrix, which arises because of different cells in configuration space. Figure 1 shows one of the typical relaxation processes in the tandem mirror:

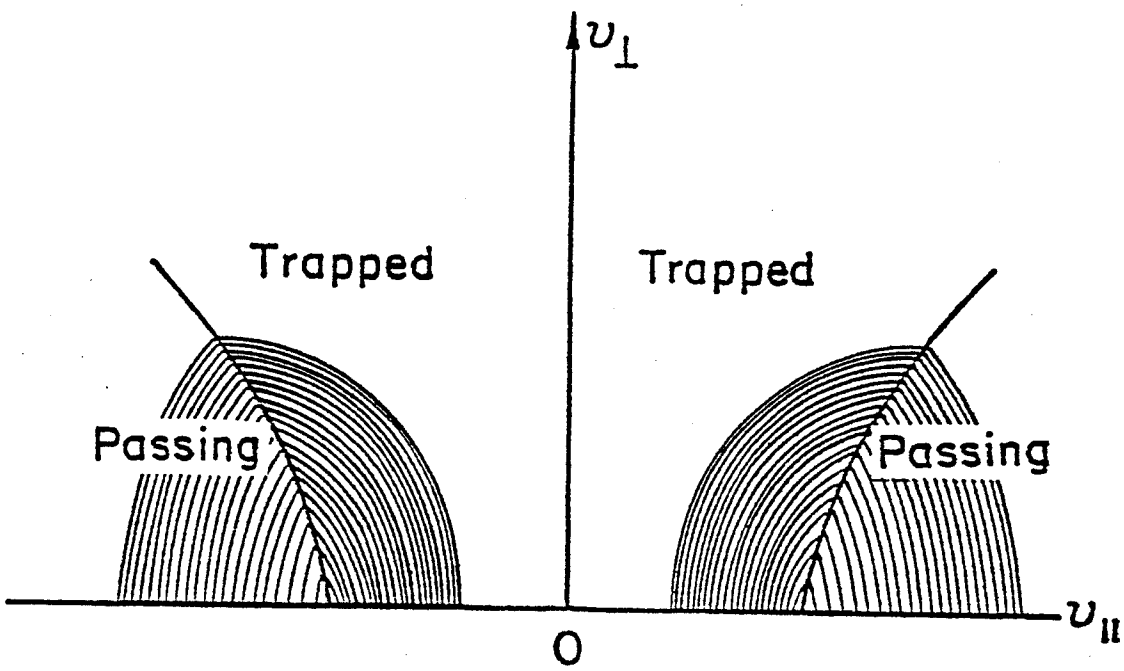

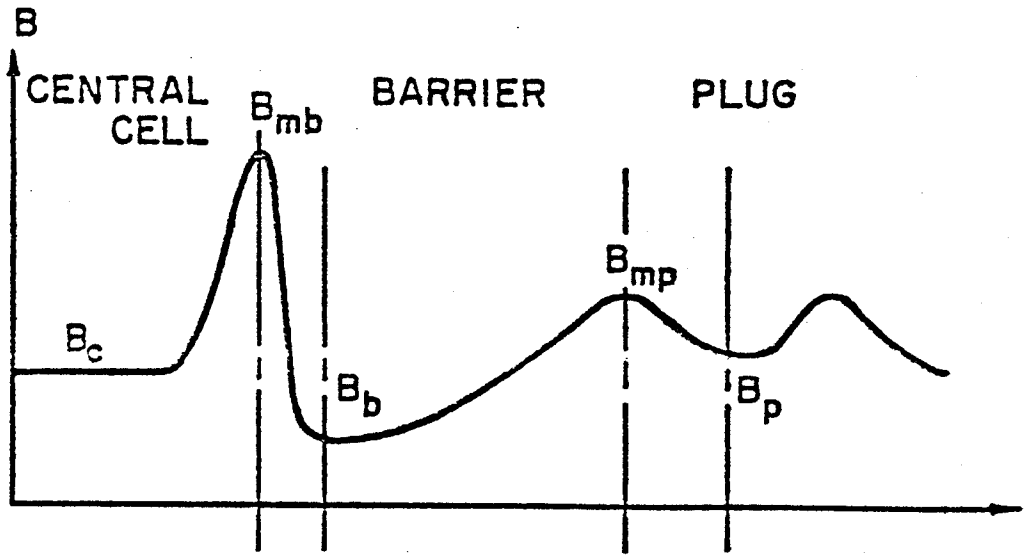

Fig. 1. The trapping process in a thermal barrier.

the trapping process in a thermal barrier. The thermal barrier is formed by a magnetic peak B_{mb} and a magnetic dip B_b, and by a potential dip ϕ_b. These parameters (the mirror ratio, B_{mb}/B_b, and the potential, ϕ_b) will determine the shape of the separatrix between the passing region and the trapped region in velocity space. The passing region is filled with the plasma which can pass through the central cell. Because of pitch angle scattering or energy slowing down, these passing ions can become trapped in the thermal barrier. This is a type of t_{ii}-scale process. Once this relaxation process reaches its equilibrium, that is, the trapped particles fill up the barrier region, the potential dip disappears; then, the rapid t_{ee}-scale process would evolve since the isolation between the hot electrons in the plug and cooler electrons in the central cell would be lost. Pumping out the trapped ions will maintain this isolation; therefore, the necessary external pumping power is determined by these t_{ii}-scale trapping processes.

In a tandem mirror reactor, the barrier pumping power is one of the major input powers. So the trapping current is one of the critical issues [3]; any substantial increase in the trapping current is intolerable. However, all tandem mirror reactor conceptual designs are based on an empirical fit of the trapping current obtained from a series of Fokker-Planck numerical code calculations. These empirical fits are obtained from calculations using a square magnetic well. Recently Futch and LoDestro [4] showed an important result for the non-square well cases; the trapping current may increase by a factor

of 2-5 in a non-square well case, compared with the corresponding square well case.

It is clear that a better understanding of this trapping process is not only crucial for the prospects of tandem mirrors, but also significant for the current conceptual design of the tandem mirror reactor.

1.2 Previous Work

A series of work has been done for the calculation of the current across the separatrix in velocity space. Here we concentrate on analytical attempts at solving the Fokker-Planck equation. Two years before the tandem mirror idea was proposed, there was an analytical calculation of the electron endloss from a magnetic mirror with electrostatic potential effects. Pastukhov (1974 [5]) solved the Fokker-Planck equation analytically to obtain the particle and power loss out the ends. At that time, the motivation was to save computer time since the time step for an electron equation is much shorter than that for an ion equation. It is too expensive to solve ion and electron equations numerically with the same time step. So the Fokker-Planck equation for electrons was selected to be solved analytically. However, the method is also valid for the ion equation. A tricky point in Pastukhov's calculation is to assume a fictitious source inside the loss cone which will produce a new zero boundary (i.e., the boundary on which the distribution function is zero). The new zero boundary overlaps with the real loss cone boundary at only one point -- the tip of the loss cone boundary -- where the curva-

tures for both boundaries are made to be equal. No one knew how much change in endloss is caused by this replacement in the boundary condition. Soon after the tandem mirror idea was proposed, Chernin and Rosenbluth (1978 [6]) used a variational method to check Pastukhov's analytical solution. Although Chernin and Rosenbluth's analytical solution is not as good as Pastukhov's, their calculation shows that the result is not very sensitive to the change of the boundary. At the same time Chernin and Rosenbluth corrected an error of a factor of 2 in Pastukhov's original expression. Since then, the Pastukhov formula was confirmed and extended to arbitrary magnetic field profile cases by Cohen and Rensink [7]. Nevertheless, the error between the numerical code result and Chernin and Rosenbluth's analytical expression is about 30%. The reason is that their expansion is based on Legendre polynomials, which is not inherent in the physics of the problem, so there is not a dominant term to be selected. When Chernin and Rosenbluth selected the largest term, the remaining terms were only smaller by a factor of $(\ln X_0/(\ln R + \ln X_0))^2$; (R is the mirror ratio, X_0 is the ratio of potential to temperature, $e\phi/T$). Catto and Bernstein [8] developed a new variational scheme, which kept the intrinsic nature of the physics. They gave up the Legendre polynomials and introduced a curvilinear coordinate, which has the coordinate line asymptotically parallel to the loss-cone boundary. Therefore their trial function for variational calculations is closer to the real solution. The agreement with the numerical code calculation is reasonably good.

From Pastukhov to Rosenbluth, to Catto and Bernstein there are some common features. Despite their differences, they all use three steps to solve the Fokker-Planck equation: (i) the linearization, (ii) the fictitious source, (iii) and an analytical method in solving the ordinary differential equation.

(i) The linearization has special meaning in this case. In general, the Fokker-Planck equation can be written as

$$\frac{\partial f_T}{\partial t} = -\nabla \cdot \vec{I}(f_F, f_T) + S \qquad (1.1)$$

where the collisional current, $\vec{I}(f_F, f_T)$ in velocity space is a bi-linear function of the test particle distribution function, f_T, and the field particle distribution, f_F. This is because $\vec{I}$ involves the diffusion tensor $\vec{\vec{D}}$ and the dynamical friction $\vec{A}$, both of which depend on f_F (for ion-ion collisions, $f_F = f_T$). Here S is the source density and ∇ is the gradient operator in velocity space. All these authors assumed a high mirror ratio ($R \gg 1$) and deep potential well ($e\phi/T \gg 1$); then the source term is a small perturbation term, since the endloss does not affect the total distribution very much. We may write

$$f_F = f_o + f_1 \qquad (1.2)$$

and

$$f_T = f_o + f_1 \qquad (1.3)$$

where f_o is the source-free zero order solution, and f_1 is the perturbation distribution function caused by the source. In a general case, we often write

$$\vec{I}(f_o+f_1,f_o+f_1) = \vec{I}(f_o,f_o) + \vec{I}(f_o,f_1) + \vec{I}(f_1,f_o) + \vec{I}(f_1,f_1) \qquad (1.4)$$

where $\vec{I}(f_F,f_T)$ is linear with respect to f_F or f_T, respectively. Usually, linearization means that we drop the $\vec{I}(f_1,f_1)$ term only; however, we drop the $\vec{I}(f_1,f_o)$ term also in the linearization of the Fokker-Planck equation. The reason is as follows: $\vec{I}(f_F,f_T)$ is dependent on f_F and f_T in two different ways. The general collisional current is

$$\vec{I}(f_F,f_T) = \vec{A}(f_F)f_T - \vec{\vec{D}}(f_F) \cdot \nabla f_T \ . \qquad (1.5)$$

$\vec{I}$ is sensitive to both the density and the shape of the "test particle distribution function," but is sensitive to only the density of "the field particle distribution function." This is because after the integration to get $\vec{A}$ or $\vec{\vec{D}}$, the shape of the field particle distribution function is no longer important. All those authors are using the dimensionless equation, which means that the normalized current is

$$\hat{\vec{I}} = (1/N^2)\ \vec{I}(f_F,f_T) \ . \qquad (1.6)$$

The effect of the density, N, has been already extracted, so the normalized current $\hat{\vec{I}}$ is approximately independent of the density of both f_F and f_T, and is only dependent on the shape of f_T. Therefore,

$$\hat{\vec{I}}(f_o+f_1,f_T) = \hat{\vec{I}}(f_o,f_T) \ . \tag{1.7}$$

This is the essence of the isotropic approximation for the Rosenbluth potentials. This is why we drop the third term in Eq. (1.4). In fact, it is correct only for the normalized diffusion current; i.e. $f_o + f_1$ and f_o correspond to the same density in the two cases.

(ii) The source is always needed to maintain a steady endloss current. After the normalization, the source will not affect the density, but the shape of the distribution function, which may be expressed as a ratio of the distribution function to the Maxwellian distribution function: $h = f/f_M$. h is zero on the loss-cone boundary and approaches one in most of the confinement region. Since the endloss current is assumed to be very small, the bulk of the plasma is not disturbed very much. In other words h is assumed to be very close to 1 no matter where the source is, so the effect of the source on the shape of the distribution is expressed by $h = 0$ on the boundary or $\nabla h \neq 0$ near the source and the boundary. Pastukhov used a fictitious source inside the loss-cone region to make $h = 0$ on a boundary which is close to the real boundary. Chernin and Rosenbluth put a real source in the low energy region and put emphasis on the $\nabla h \neq 0$ region in the vicinity of the source. Catto and Bernstein put

a real source in the low energy region also, but addressed the $\nabla h \neq 0$ region in the vicinity of the loss-cone boundary. At any rate, with the help of the source, the steady state equation is set up, and different methods are used to solve this equation analytically.

(iii) Analytical solution: after the linearization and the normalization, the task is reduced to determining the shape of the distribution function h, which is mainly specified by the boundary condition where $h = 0$. Thus the problem becomes that of figuring out the necessary loss current to fit this boundary condition. In order to simplify the problem, the boundary condition is simplified in various ways. The Pastukhov method assumes a new boundary which overlaps with the real loss-cone boundary at the tip and has the same curvature there (Fig. 2). This gives two equations to fix the position and the intensity of the necessary fictitious source.

Chernin and Rosenbluth also changed the shape of the boundary to facilitate their expansion in Legendre polynomials. They found the zero boundary would produce a nonzero derivative ∇h on the surface surrounding the low energy source (Fig. 3), which is in balance with the endloss current.

Catto and Bernstein kept the real shape of the boundary and simplified their calculation by a new coordinate system which fits the real shape of the loss-cone boundary. They used the contour of constant distribution function h to specify the shape of the distribution in the vicinity of the loss-cone, where $\nabla h \neq 0$ (Fig. 4). A variational method was used to find a solution in the transition

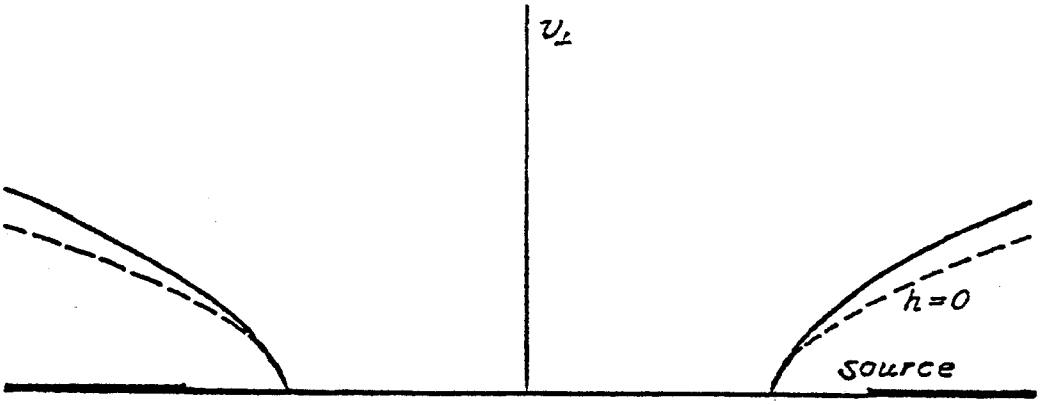

Fig. 2. Pastukhov's boundary and source.

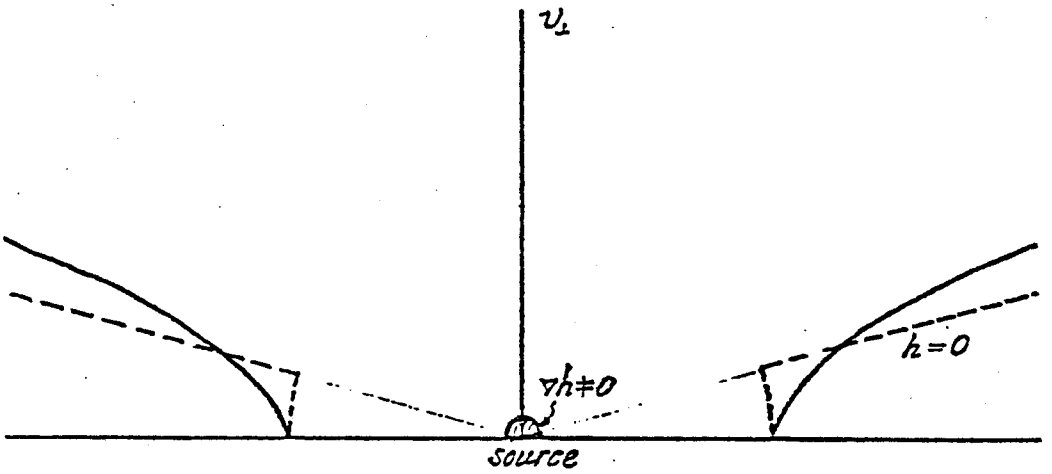

Fig. 3. Chernin and Rosenbluth's boundary and source.

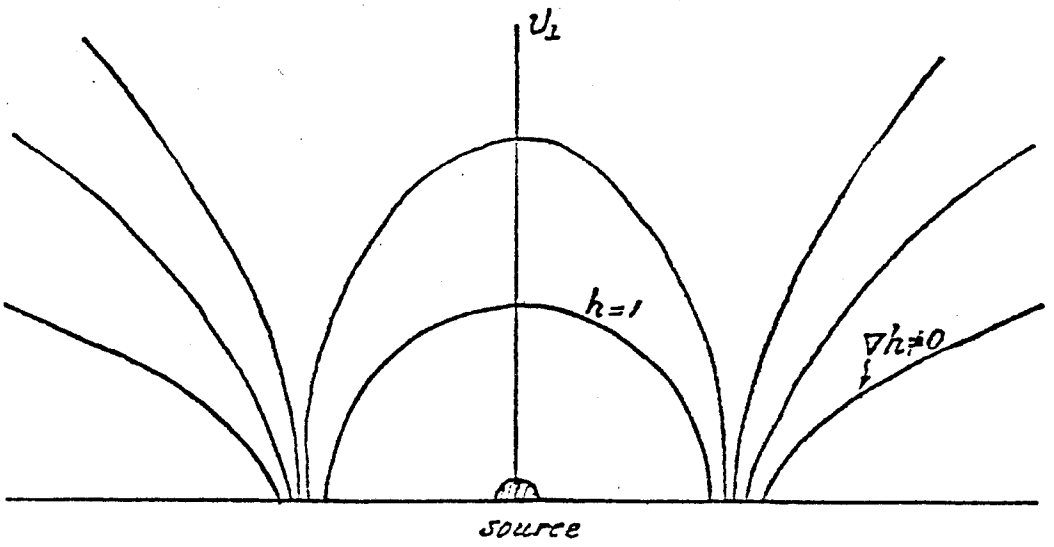

Fig. 4. Catto and Bernstein's boundary and source.

region which would give a divergence free flow and match the boundary where h = 0 and h = 1.

In summary, the contours of constant distribution function are drawn in Fig. 5. The errors of these analytical calculations in comparison with the numerical code results are about 10-30%. Cohen [7] and Rensink made a series of calculations to check the linearization assumption and the approximation in the boundary condition. It shows that the linearization is quite reasonable. The nonlinear code calculation gives an improvement of about 2%. The Pastukhov expression gives the better fit with the code calculation of within ±20%. Considering that the error caused by the discrete grids is about ±7%, we see the accuracy of the Pastukhov method.

Up to now all three aforementioned methods were tested only in the square magnetic well cases, although both analytical and numerical calculations for an arbitrary magnetic field profile are possible.

These three methods commonly use the assumption of a Maxwellian field particle distribution function, which is correct as long as a deep well configuration is assumed ($\phi/T \gg 1$). In the thermal barrier pumping problem, however, we have a non-Maxwellian field particle distribution function. The bulk of the plasma is a result of the diffusion process (Fig. 1). About one-half of the density (trapped particle density) is directly related to the trapping current. This is totally different from the case of the endloss from a deep well, where the endloss current does not substantially affect

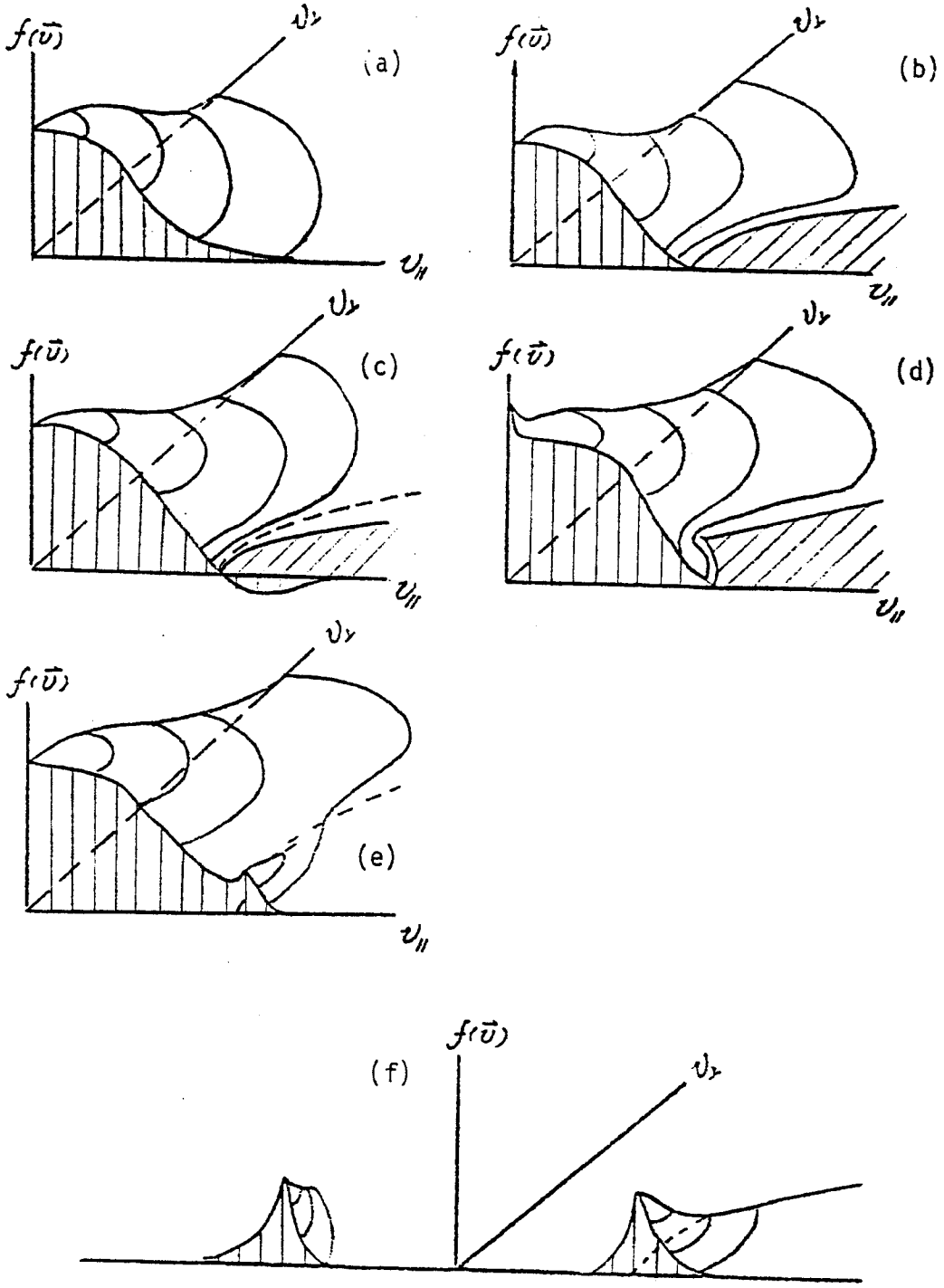

Fig. 5. Contours of the constant distribution function for different cases. (a) Pure Maxwellian. (b) Maxwellian with a real loss-cone. (c) Pastukhov fictitious loss-cone. (d) Chernin and Rosenbluth's approximate loss-cone. (e) Weak pumping in a thermal barrier. (f) Strong pumping in a thermal barrier.

the bulk of the plasma. Does the linearization still work in this case? It was not clear when we started our research.

LoDestro [9] and Futch and LoDestro [4] did a series of numerical code calculations for the thermal barrier trapping process. This is a kind of nonlinear calculation, since the Fokker-Planck coefficients are calculated step by step. Starting from pure passing particles as an initial condition, the code runs to a steady state equilibrium where the diffusion across the passing-trapped boundary is balanced by the charge exchange process (neutral beam pumping). After a number of code calculations, they found an empirical fit for the trapping current J_t. In 1979 [10] the formula was

$$J_t(z) = \{(N_p(z))^2/(5.5 \times 10^9\ T_e^{3/2})\}\{1 + 0.55\ R(z)\}\ . \qquad (1.8)$$

Here, T_e and N_p are the temperature (in keV) and density of the passing particles, $R(z)$ is the local mirror ratio inside the thermal barrier, and $J_t(z)$ is the corresponding local trapping current. In 1980 [11] this formula became

$$J_t = \frac{N_p^2}{2.3 \times 10^9\ T_e^{3/2}}\ (1 + 0.2\ R_b)\ . \qquad (1.9)$$

In 1982 [4] more calculations gave a new fit of

$$J_t = 0.935\ g_b\ (1 + 0.0441\ R_b)\ Y^{0.7}\ N_p/(N_b t_p) \qquad (1.10)$$

for deuterium plasma. Here

$$N_b t_p = 6.27 \times 10^{11} T_p^{3/2}/\ln \Lambda \qquad (1.11)$$

and

$$\ln \Lambda = 34.9 - 0.5 \ln(N_b/(ET_e)) \; . \qquad (1.12)$$

E is the average ion energy at the bottom of the well; T_e is the electron temperature; the energy and temperatures are in keV; N_b is the total density at the bottom of the well. $g_b = N_b/N_p$ is the pumping factor. Also

$$Y = \nu(N_b t_p)/N_p \; . \qquad (1.13)$$

Here, ν is the beam pumping rate in sec^{-1}. The changes and the complicated form mean that a better understanding of the trapping process is important. Numerical calculations [4] showed that a factor of 2-5 is introduced for different profiles of the magnetic field. Thus an analytical expression based on a better understanding is especially needed. All these numerical code calculations, including Rognlien's Monte-Carlo calculations [14], provide a basis on which to build some analytical model for the barrier pumping process.

In 1980 (Li and Emmert [13]) a model for ion trapping in a thermal barrier was assumed for the passive pumping scheme. A separable form of the distribution

$$f(E,\theta) = F(\theta)\ \exp(-E/T)$$

was used to describe the trapped particles. The energy dependence was assumed to be Maxwellian; the pitch angle, θ, dependence satisfies the pitch angle scattering equation with a Lorentz operator. The boundary condition was to match the Maxwellian distribution of the passing particles to the real boundary shape. The passive pumping condition was described by a zero boundary at a specific spatial point specified by B_0,ϕ_0 (the magnetic field and potential at the passive pumping point). This model was used to calculate the pumping current and the potential profile [14]. In 1981 [15] a two step model was suggested to describe the neutral beam pumping in a thermal barrier. A hyper-geometric series (generalized Legendre polynomials) was used for the description of the pitch angle dependence. An $\exp(-|E|)$ dependence with $E = 0$ at the tip of the passing-trapped boundary was assumed for the energy dependence. The contours of constant distribution function obtained are very similar to the numerical code calculations (Fig. 6). Based on the contours of a constant distribution function, Cohen [16] proposed another distribution function for the trapped particles:

$$f_t = N_0\ (m/(2\pi T))^{3/2}\ \exp\{(E - a\mu)/((a - 1)T)\}\ . \qquad (1.15)$$

Here E and μ are the energy and the magnetic moment of the particles; a is a phenomenological parameter to describe the pumping effect

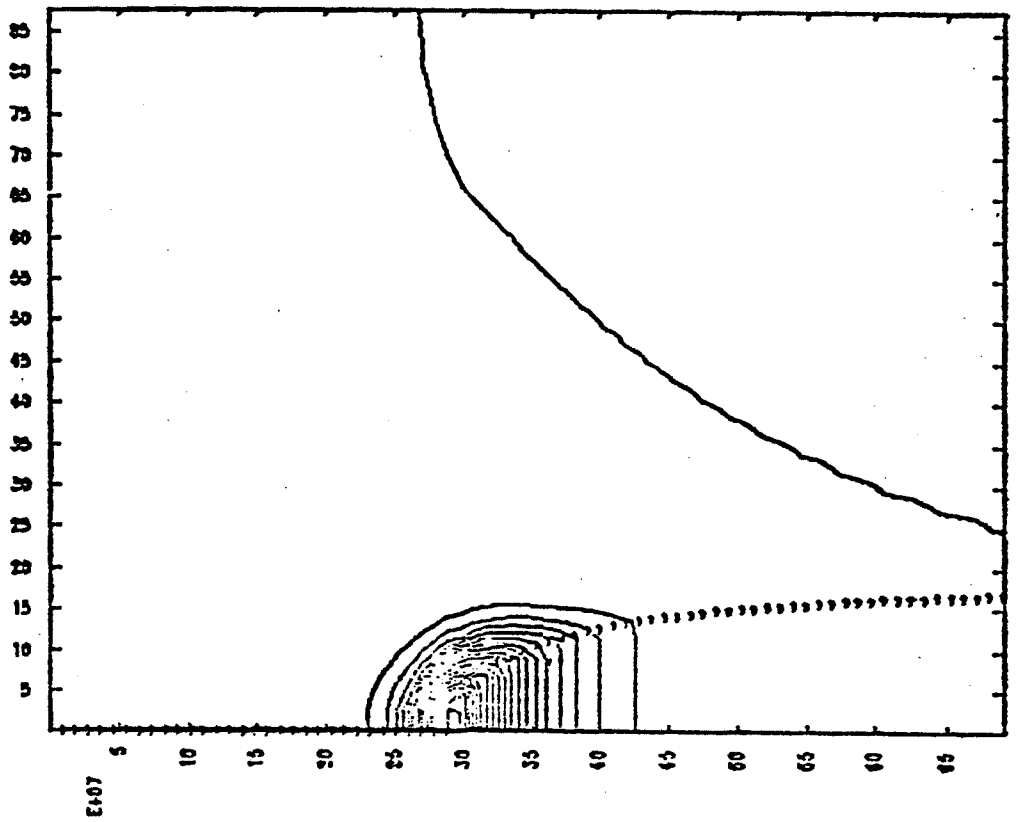

Fig. 6. (a) Contours of the constant distribution function from the two step model.

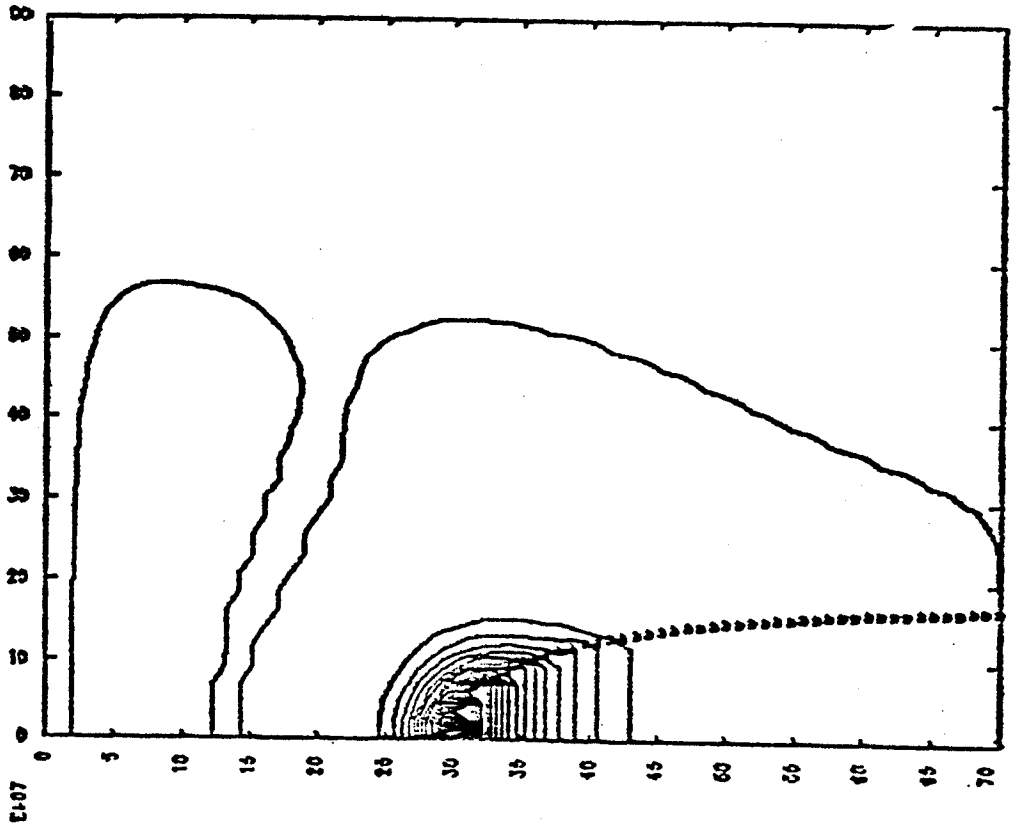

Fig. 6. (b) Contours of the constant distribution function from the bounce average code.

(a = 1 corresponds to perfect pumping, a = 0 corresponds to pure Maxwellian, i.e. no pumping at all). This form is used by Pearlstein [17] for the calculation of the potential profile in the barrier in a sloshing-ion A-cell. Although the contours of this distribution function are not really similar to the numerical code results (Fig. 7), it is accepted because it is less likely to lead to discontinuities in the potential. In 1982 [18] Carrera and Callen proposed a solution using the conical function for the description of the pitch angle dependence. The boundary is deformed to facilitate an analytical treatment (Fig. 8). After the integration in velocity space, the ratio of the density of trapped particles to passing particles was calculated. Once the total density N_b is input, the trapped particle density, and therefore the trapping current, can be calculated. When the mirror ratio is large, the deformation of the boundary does not cause a big error; the results agree with Futch and LoDestro's calculation within 20% for the trapping current.

The various aforementioned methods for the barrier trapping process are all based on pitch angle scattering. Energy diffusion is ignored. However, energy diffusion may play an important role when the mirror ratio is low. As we pointed out in the two step model, there is always a region near the mirror throat where the mirror ratio is low but the density is high. Energy diffusion in that region must be dominant. In fact the starting point of the variational calculation which we present in this thesis was just a trial to include this energy diffusion effect.

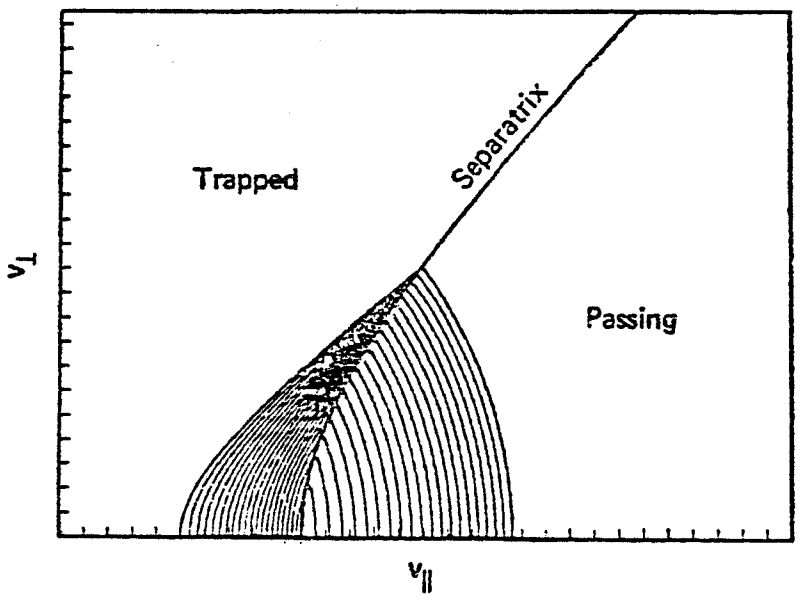

Fig. 7. Contours of the constant distribution function from Cohen's formula (Eq. (1.15)).

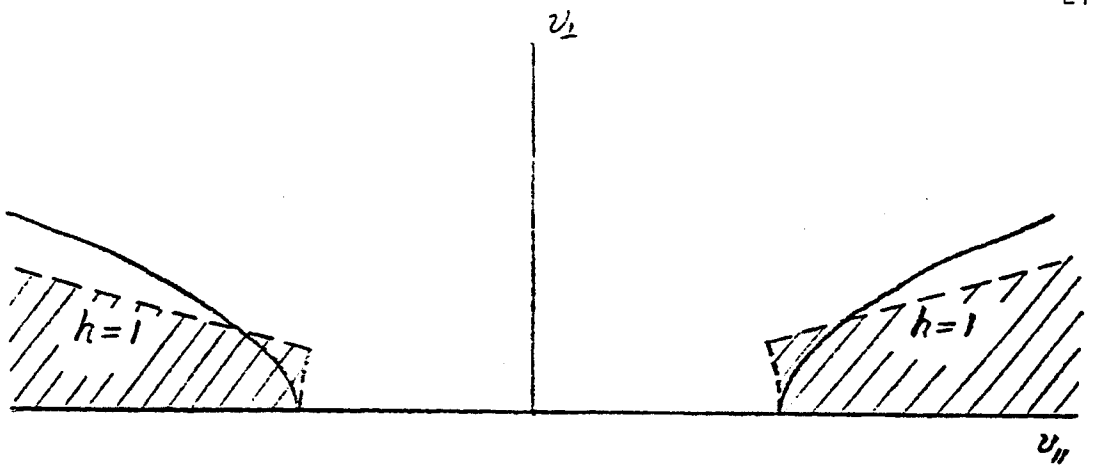

Fig. 8. Deformed boundary for the thermal barrier calculation in Ref. 18.

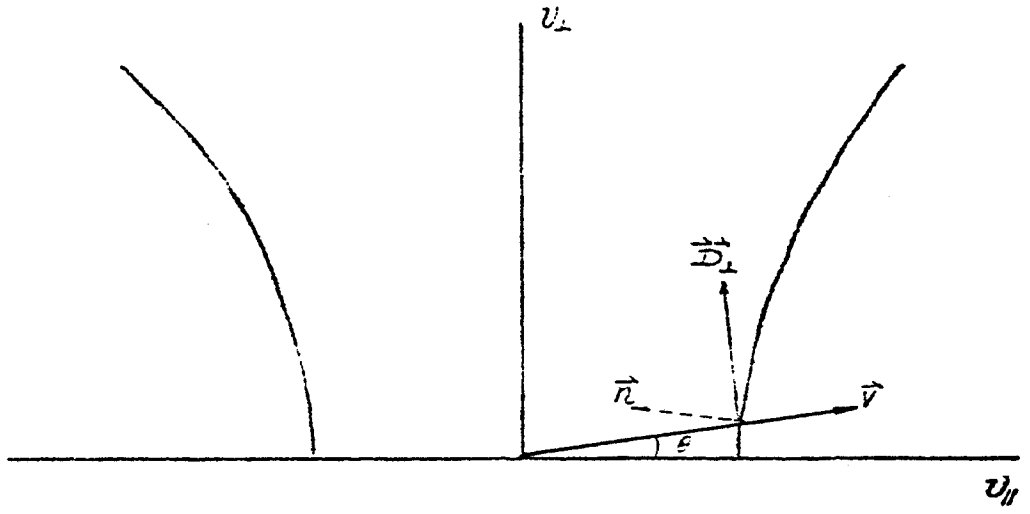

Fig. 9. The role of energy diffusion and pitch angle scattering at low mirror ratio.

2. PHYSICS

2.1 Energy Diffusion

If we consider the velocity space for the low thermal barrier mirror ratio case, we see that the surface of the boundary near the tip is approximately perpendicular to the vector $\vec{v}$ (Fig. 9). The diffusion tensor $\vec{\vec{D}}_{\perp}$ will contribute little to the current across the boundary; $\vec{\vec{D}}_{\parallel}$ and $\vec{A}$ (the dynamic friction tensor) will play the dominant role. Only at points far away from the tip does the $\vec{\vec{D}}_{\perp}$ play a dominant role. However, the distribution function inside the passing region is approximately Maxwellian, since the central cell has greater volume and density than the thermal barrier. The distribution function drops dramatically at points far away from the tip of the boundary. If we want a good calculation of the trapping current, we must take into account the energy diffusion process.

2.2 Two Group Approximation in a Square Well

Once we recognize the importance of the energy diffusion process, an approximation can be made using the "Lorentz operator" for the energy diffusion process. Usually, the Lorentz operator is used for the pitch angle scattering process; the pitch angle, θ, denotes the angle between the velocity vector $\vec{v}$ and the magnetic field. However, we know that the relative velocity between the test particle and the field particle, $(\vec{v} - \vec{v}')$, plays the key role in determining these Coulomb interactions. The relative velocity, and not the absolute velocity $\vec{v}$, should have been considered. According

to their relative velocities, the passing particles can be divided into two groups: passing towards the left ($v_{\parallel} < 0$) and passing towards the right ($v_{\parallel} > 0$). When the potential dip of the thermal barrier, ϕ_b, is much greater than the temperature of the passing particles, T_p, the Coulomb interaction between the particles in the same group is much greater than the Coulomb interaction between the particles in different groups, since their relative velocities differ by a factor of $(\phi_b/T_p)^{1/2}$. Typically, a particle moving towards the right will interact with the particles concentrated at the right tip of the boundary. Their relative velocity is denoted by $\vec{v}_1$ (Fig. 10). The pitch angle of this velocity is θ_1. Now we can say that the pitch angle scattering of this vector $\vec{v}_1$ will dominate the current across the boundary. Then we may use the "Lorentz operator" to describe this pitch angle scattering in the co-moving frame, which is equivalent to an energy diffusion process in the laboratory frame. The key point is that this description works for both high mirror ratio, $R_b >> 1$, and low mirror ratio, $R_b \gtrsim 1$ cases.

At the same time we should check the contribution from the interaction with the group moving towards the left. Their relative velocity is designated by $\vec{v}_2$. As we described before, the energy diffusion of vector $\vec{v}_2$ can contribute to the trapping process, but we can prove that its contribution is negligible. Since Coulomb scattering in plasma is dominated by small angle scattering, the change in the momentum δp has the following relation (see Fig. 11)

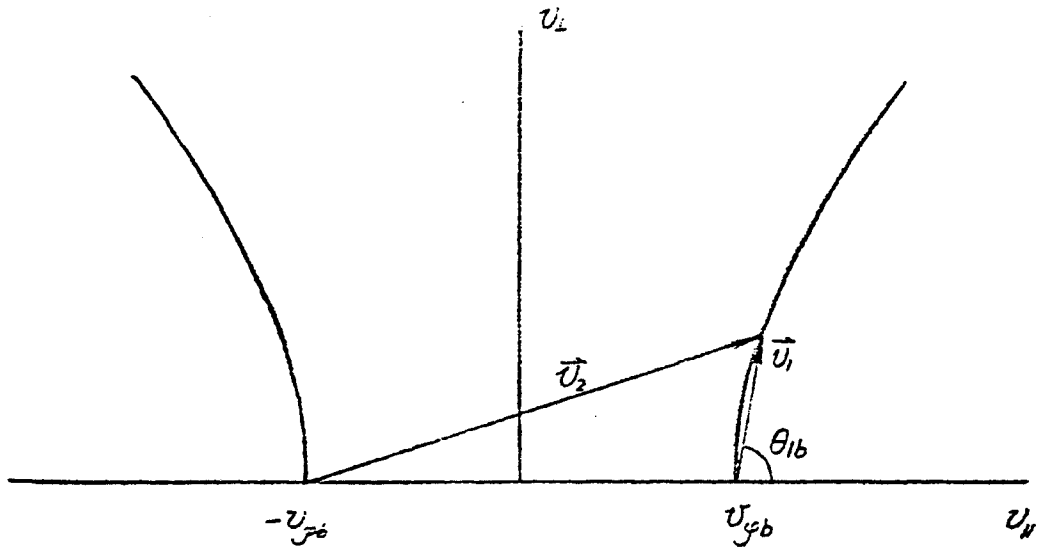

Fig. 10. Definition of the relative velocity $\vec{v}_1$ and $\vec{v}_2$.

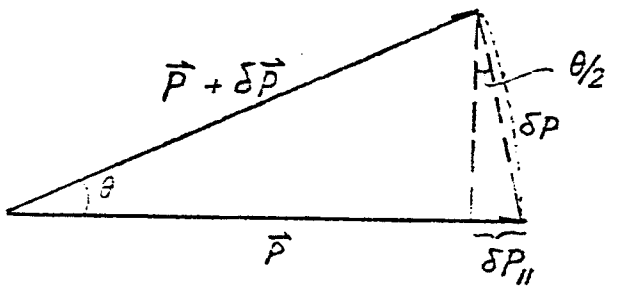

Fig. 11. The change of momentum in a Coulomb collision.

$$\delta p_{\parallel} \approx \delta p_{\perp}\, \theta/2 \approx \delta p_{\perp}\, \delta p_{\perp}/(2p) \approx (\delta p_{\perp})^2/(2p) \ . \qquad (2.1)$$

For the fast incident particles, the momentum change in Coulomb scattering is

$$\delta p_{\perp} = (2q_1q_2)/(bu) \ . \qquad (2.2)$$

Here, q_1, q_2 are the electrical charges of the test and field particles respectively, b is the impact parameter, and u is the relative speed. Hence

$$\delta p_{\perp} \propto 1/u \ , \qquad (2.3)$$

$$\delta p_{\parallel} \propto 1/(2pu^2) \propto 1/u^3 \ . \qquad (2.4)$$

So the energy diffusion process diminishes much faster than the pitch angle process when the relative speed increases. Therefore, the contribution from the left moving group is negligible; we concentrate on the contribution from the right moving group, which can be expressed by a center-shifted pitch angle scattering.

2.3 Two Sphere Model

Even if the problem is simplified from two tips to one tip, it is still difficult to write the diffusion tensors $\vec{D}$ and $\vec{A}$. In fact, we are facing a nonlinear problem: the diffusion tensors $\vec{D}$ and $\vec{A}$ are functions of the field particles which are composed of passing particles and trapped particles; inversely, the trapped particles distri-

bution function itself is a function of the diffusion tensors $\vec{\vec{D}}$ and $\vec{A}$. This difficulty may be overcome by a modified isotropic Rosenbluth potential technique [19]. A simple example can show the essentials of this technique. When we are calculating the water flow over Niagara Falls, we are concerned with the steepness of the mountain, but we are never concerned with the change of the acceleration of the gravity, $\vec{g}$, due to the shape of the mountain. Although we know that the distribution of the mass would affect the acceleration of gravity, we always use the $\vec{g}$ value of the round earth, ignoring the bumpy surface of the earth and other inhomogeneities. Because we know that the $\vec{g}$ value is determined by an integration of the distribution of the mass, the $\vec{g}$ value is not sensitive to the local topographical features. The diffusion tensors $\vec{\vec{D}}$ and $\vec{A}$, like $\vec{g}$, are dependent on an integration of the distribution function of the field particles. Although the trapped particles have a different distribution function than the passing particles, we may try to use an isotropic distribution in calculating the diffusion tensors $\vec{\vec{D}}$ and $\vec{A}$. We select the tip of the passing-trapped boundary as the center of the isotropic distribution; this is different from all the work mentioned before. Our calculation confirms this approximation a posteriori.

After the isotropic approximation of the field particle distribution function, the nonlinear problem becomes linearized. Now we are calculating the water flow without being concerned with the effect on $\vec{g}$ due to the shape of the waterfall.

2.4 Boundary Condition

However, this does not mean that we no longer need any knowledge about the shape. In fact, the water level is essential in calculating the water flow. Likewise, we should carefully specify the boundary condition on the passing-trapped boundary. At this point the trapping process in the barrier is very different from the endloss process in mirrors. In the thermal barrier we are dealing with the boundary condition at the upper reaches of a river; whereas the zero boundary condition in the mirror is at the lower reaches of a river. If the seashore is changed a little except at the reaches of the river mouth, the discharge of the river will not change very much. In contrast, if the topographical feature near the Three Gorges of the Yangtze river were changed, the discharge of the river would change greatly. Therefore, we attempt assiduously to keep the real shape of the passing-trapped boundary and keep the real value of the distribution function along the whole boundary. This is realized by a special choice of coordinates in which separability is assumed.

2.5 Neutral Beam Pumping Model

In addition, we have one more special consideration in the trapping rate calculation. There are two unknowns: the total density in the barrier, N_b, and the shape of the distribution function. In the calculation of the endloss in a mirror, the total density is fixed. Once the shape of the distribution function is fixed, the endloss current is determined also. However, in the calculation of the trapped current, the passing particle density is fixed as an input,

but the total density in the barrier (trapped particles plus passing particles) is not fixed. The total density should be obtained self-consistently with the shape of the distribution function of the trapped particles. Therefore, one more physical condition is needed to solve this trapping rate. Fortunately, the constancy of the neutral beam charge exchange rate provides a simple additional condition without our knowing the distribution function of the trapped particles. This makes it easy to have a simple analytical expression of the trapping current in a thermal barrier.

2.6 Philosophy

Lastly, one thing we would like to mention is the philosophy guiding us toward the solution. If you want to know how many people are going into a room, you just count at the door. It is not necessary to know the details inside the room. So we not only carefully deal with the boundary condition, but also keep the equation near the boundary as accurate as possible. When we look for a trial function, we watch the behavior of the solution near the boundary first.

Now let us see how this philosophy guides us in the complicated mathematics.

3. MATHEMATICS

3.1 The Variational Method

Since we have decided to keep the real shape and real value of the boundary, we need a powerful mathematical tool to cope with the complicated geometric shape. Catto and Bernstein [8] show how the variational method facilitates their calculation and how a new curvilinear coordinate system is introduced in order to keep the real boundary condition. Because the endloss current is equivalent to the stationary value of the functional, they obtained better accuracy in the endloss than in the distribution function.

When we try to use the variational method in the barrier trapping process, the first question is whether there is in fact a functional for the Fokker-Planck equation in this special case. In general, we can prove that the Fokker-Planck collisional operator is self-adjoint provided that the field particle distribution function is Maxwellian [20]. Unfortunately, in the barrier trapping process, the field particles are rather non-Maxwellian. Then the existence of the functional is an open question.

The second question which appeared is how to obtain a suitable trial function. A good first guess for the trial function is essential for a variational method. If a first guess is very close to the real solution, then only a few parameters are needed to improve this first guess in order to get a closed form analytical solution. In fact, both Chernin and Rosenbluth and Catto and Bernstein used the

variational method to solve the endloss problem. The difference between their methods is the choice of the first guess. Catto and Bernstein kept the natural boundary and let the contour of the constant distribution function follow curves similar to the boundary, so their result has better agreement with the code calculation. We try to use Catto and Bernstein's contour method, but we correct the way of introducing the variational parameter. In Catto and Bernstein's paper, the functional L(h) is a function of the unknown function h. h is a function of the new coordinate y, i.e

$$L(h) = \int dy\ p(y)\ (dh/dy)^2 \ . \qquad (3.1)$$

Here, p(y) should be independent of the function h; otherwise its Euler-Lagrange equation will not recover the Fokker-Planck equation. However, when Catto and Bernstein introduced a variational parameter Δ in the definition of the y, this made p(y) dependent on the variational parameter Δ. This dependence is not legitimate in a strict variational sense, since only the trial function of h is allowed to have a variational parameter in it. In our first paper [20] we made the same mistake as Catto and Bernstein, but we corrected it in a succeeding paper [21]. Our method is more general and has better accuracy.

3.2 The Basic Equation and Its Separable Form

In a square well approximation, the balance equation in the trapped region is

$$-\nabla \cdot \vec{I} - \nu f = 0 \ . \tag{3.2}$$

Here, f is the distribution function of the trapped particles; ν is the charge exchange pumping rate ($\nu = N_0 \langle \sigma_{cx} v \rangle$, σ_{cx} is the charge exchange cross section; N_0 is the neutral density; v is the relative velocity; ν is assumed to be a constant in the range of interest). $\vec{I}$ is the Fokker-Planck collisional current [22]:

$$\vec{I} = \vec{A}(f^*)f - \vec{\vec{D}}(f^*) \cdot \nabla f \ . \tag{3.3}$$

Here, $\vec{A}(f^*)$ and $\vec{\vec{D}}(f^*)$ are the dynamic friction tensor and diffusion tensor, respectively. f^* is the distribution function of the field particles.

$$\vec{A}(f^*) = (4\pi e^4/m^2) \ln \Lambda \int f^*(\vec{v}')(\vec{v}' - \vec{v})/|\vec{v} - \vec{v}'|^3 \, d^3v' \ , \tag{3.4}$$

$$\vec{\vec{D}}(f^*) = (2\pi e^4/m^2) \ln \Lambda \, \nabla \nabla \int f^*(\vec{v}')|\vec{v}' - \vec{v}| \, d^3v' \ . \tag{3.5}$$

Here, e and m are the electrical charge and mass of the particles, respectively, and $\ln \Lambda$ is the Coulomb logarithm.

Since the unknown distribution function, f, per se is the field particle distribution function, f^*, also, the basic equation is a nonlinear integro-differential equation for f. Now we assume a separable form of the distribution function f, i.e.

$$f(\vec{v}) = R(v_1)\, Z(\eta) \ . \tag{3.6}$$

Here, $\vec{v}_1$ is a new vector starting from the extreme tip of the right passing-trapped boundary; η is a new variable which is defined to be zero on the boundary. Now $R(v_1)$ represents the isotropic part of the distribution function $f(\vec{v})$ (isotropic around the right tip!), and $Z(\eta)$ represents the anisotropy. Since we know that $f(\vec{v})$ should be equal to the Maxwellian passing particle distribution function on the passing-trapped boundary, we can solve the $R(v_1)$ first by setting $Z\big|_{\eta=0} = 1$. Then, the unknown function becomes $Z(\eta)$ with a boundary condition

$$Z(0) = 1 \ . \tag{3.7}$$

$Z(\eta)$ satisfies the equation:

$$\nabla \cdot (R\vec{\vec{D}} \cdot \nabla Z) - \nabla \cdot (\vec{t} Z) - \nu R Z = 0 \ . \tag{3.8}$$

Here,

$$\vec{t} = \vec{A} R - \vec{\vec{D}} \cdot \nabla R \ . \tag{3.9}$$

It should be noted that the equation for $Z(\eta)$ is self-adjoint as long as the second term, $\nabla \cdot (\vec{t} Z)$, can be neglected. We should study the properties of the vector $\vec{t}$.

As mentioned before, the diffusion tensors $\vec{A}(f^*)$ and $\vec{\vec{D}}(f^*)$ might be approximated by a replacement of $f^*(\vec{v})$ with its isotropic

part $R(v_1)$ around the tip. The contribution from the left tip is totally ignored, and the effect of anisotropy due to $Z(n)$ is neglected also. Under this single sphere approximation, the vector $\vec{t}$ is in the direction of $\vec{v}_1$. Furthermore, we may obtain the isotropic part, $R(v_1)$, as

$$\begin{aligned} R(v_1) &= G \exp\{-(\tfrac{1}{2} m(\vec{v}_{\phi b} + \vec{v}_1)^2 - \phi_b)/T_p\} \\ &= G \exp\{-(m(v_1^2 + 2v_1 v_{\phi b} \cos\theta_{1b})/(2T_p))\} \\ &= G \exp\{-(v_1/v_t)^2 - 2(v_1/v_t)(v_{\phi b}/v_t)\cos\theta_{1b}\} . \end{aligned} \tag{3.10}$$

Here, G is a constant determined by the passing particle density, N_p, i.e.

$$G = (N_p/H)(m/(2\pi T_p))^{3/2} \tag{3.11}$$

$$H = \exp(y)\,\mathrm{erfc}(\sqrt{y}) - \sqrt{1/z}\,\exp(zy)\,\mathrm{erfc}(\sqrt{zy}) \tag{3.12}$$

$$y = \phi_b/T_p \;;\quad z = R_b/(R_b - 1) . \tag{3.13}$$

For the case of large mirror ratio, R_b, and large potential dip, ϕ_b,

$$H \to (1/R_b)\sqrt{(T_p/(\pi\phi_b))} . \tag{3.14}$$

θ_{1b} is the pitch angle of the vector $\vec{v}_1$ when $\vec{v}_1$ is on the boundary. Hence,

$$\cos\theta_{1b} = (1/R_b)\{-(v_{\phi b}/v_1) + \sqrt{(v_{\phi b}/v_1)^2 + R_b(R_b - 1)}\} . \tag{3.15}$$

As we know, most of the particles are concentrated at the tip, where $v_1 << v_{\phi b}$; hence, $\cos \theta_{1b} \rightarrow ((v_1/2v_{\phi b})(R_b - 1))$

$$R(v_1) = G \exp\{-R_b(v_1/v_t)^2\} , \tag{3.16}$$

which is a "Maxwellian distribution" with center shifted to $\vec{v} = \vec{v}_{\phi b}$. We might guess that the tensor $\vec{t}$ is very close to zero in the region of interest. In reality, if we use $R(v_1)$ instead of f* in the $\vec{A}(f^*)$ and $\vec{\vec{D}}(f^*)$ expressions, and if we let $R(v_1)$ equal a pure Maxwellian center-shifted distribution, then $\vec{t} = 0$. Although $R(v_1)$ is not a pure Maxwellian, there is another factor which helps to suppress the contribution from the second term of Eq. (3.8) in the passing-trapped boundary. Let us introduce a new coordinate system, (v_1,η,ψ), with Jacobian $J(v_1,\eta)$. Multiplying Eq. (3.8) by $J(v_1,\eta)$ and integrating over $dv_1 d\psi$, we have

$$\iint dv_1 d\psi\ J\nabla\cdot(R\vec{\vec{D}}\cdot\nabla Z) - \iint dv_1 d\psi\ J\nabla\cdot(\vec{t}Z) - \iint dv_1 d\psi\ J\nu RZ = 0 . \tag{3.17}$$

Here, ψ is the azimuthal angle in velocity space. Using the generalized Gaussian Theorem (see Appendix I), we have

$$\begin{aligned} \iint dv_1 d\psi\ J\nabla\cdot(R\vec{\vec{D}}\cdot\nabla Z) &= \frac{d}{d\eta}\left\{\iint dv_1 d\psi\ J\nabla\eta\cdot R\vec{\vec{D}}\cdot\nabla Z\right\} \\ &= \frac{d}{d\eta}\left\{p(\eta)\frac{dZ}{d\eta}\right\} \end{aligned} \tag{3.18}$$

where $$p(\eta) = \iint dv_1 d\psi \; J\nabla\eta \cdot \vec{\vec{RD}} \cdot \nabla\eta \; , \tag{3.19}$$

and

$$\iint dv_1 d\psi \; J\nabla\cdot(\vec{t}Z) = \frac{d}{d\eta} \left\{ \iint dv_1 d\psi \; J(\nabla\eta\cdot\vec{t})Z \right\} = \frac{d}{d\eta} \left\{ q_2(\eta)Z(\eta) \right\} \tag{3.20}$$

where $$q_2 = \iint dv_1 d\psi \; J(\vec{t}\cdot\nabla\eta) \; . \tag{3.21}$$

The equation becomes

$$d/d\eta \; \{p(\eta)dZ/d\eta\} - d/d\eta \; \{q_2(\eta)Z(\eta)\} - q_0(\eta) = 0 \; . \tag{3.22}$$

where $$q_0(\eta) = \iint dv_1 d\psi \; J\nu R \; . \tag{3.23}$$

The "watch door" philosophy guides us to address the boundary layer, where

$$(\vec{t}\cdot\nabla\eta)_{\eta\to 0} \sim 0 \; . \tag{3.24}$$

We may neglect the q_2 term in Eq.(3.22); consequently, we get

$$d/d\eta \; \{p(\eta)dZ/d\eta\} - q_0(\eta)Z(\eta) = 0 \; , \tag{3.25}$$

which is self-adjoint. The boundary condition for $Z(\eta)$ is

$$Z(0) = 1 \tag{3.26}$$

$$\left.\frac{dZ}{d\eta}\right|_{\bar{\eta}} = 0 \ . \tag{3.27}$$

$\bar{\eta}$ is assigned to the midplane in velocity space. Because of left-right symmetry, we obtain the second boundary condition, Eq. (3.27).

3.3 The Functional and Its Physical Meaning

The equation (3.25) now is in a Sturm-Liouville form. Its functional is

$$L(Z) = \int d\eta \ \{p(\eta)(dZ/d\eta)^2 + q_0(\eta)Z^2(\eta)\} \ . \tag{3.28}$$

The variation of L(Z) recovers the Euler-Lagrange equation (3.25).

It is interesting to note that the stationary value of the functional is just the trapping current across the boundary. Substituting Eq. (3.25) into (3.28), we have the stationary value of the functional:

$$\begin{aligned} L(Z)\big|_{st.} &= \int d\eta\{p(\eta)(dZ/d\eta)^2 + d/d\eta\{p(\eta)dZ/d\eta\}\ Z(\eta)\} \\ &= \int d\eta\ d/d\eta\{p(\eta)(dZ/d\eta)Z(\eta)\} \\ &= \{p(\eta)(dZ/d\eta)Z(\eta)\}_0^{\bar{\eta}} = -p(0)(dZ/d\eta)\big|_{\eta=0} \ . \end{aligned} \tag{3.29}$$

On the other hand, the total current across the boundary is

$$J_t = \int \nu f \, d^3v = \int \{\nabla\cdot(R\vec{\vec{D}}\cdot\nabla Z) - \nabla\cdot(\vec{t}Z)\} \, d^3v$$

$$= 2\{\int dv_1 d\psi \, J\nabla\eta\cdot(R\vec{\vec{D}}\cdot\nabla Z) - \int dv_1 d\psi \, J\nabla\eta\cdot(\vec{t}Z)\}_o^{\bar{\eta}} \qquad (3.30)$$

$$= 2\{p(\eta) \, dZ/d\eta - q_2(\eta) \, Z(\eta)\}_o^{\bar{\eta}} .$$

Because of pumping, $q_2(\eta)Z(\eta)\big|_{\bar{\eta}}$ is very small, and since $q_2(0) \approx 0$ as discussed before, we have

$$J_t \approx -2p(0)(dZ/d\eta)_{\eta=0} = 2\{L(Z)\}_{st.} \qquad (3.31)$$

This equation helps us to obtain the trapping current, J_t, with better accuracy, although the first guess for the distribution function $Z(\eta)$ may be not very precise.

3.4 The Definition of η and the Trial Function

Up to now the equation for $Z(\eta)$ and its functional are a kind of general formulation. We have not yet specified η and determined how to choose a trial function. What we know is the definition of $Z(\eta)$

$$Z(\eta) = f(\vec{v})/R(v_1) \qquad (3.32)$$

and $\eta = 0$ on the passing-trapped boundary. If we start the real calculation, we need an expression for η to calculate the Jacobian $J(\eta,v_1)$ and a rough analytical form for $Z(\eta)$ to guess the trial function.

In order to realize this, we go back to the original equation

$$\nabla\cdot(R\vec{\vec{D}}\cdot\nabla Z) - \nabla\cdot(\vec{\vec{t}}Z) - \nu R = 0 \ . \tag{3.33}$$

Simply assuming that R is a pure Maxwellian distribution with its center shifted to $\vec{v} = \vec{v}_{\phi b}$, and approximating the field particle distributions in the $\vec{\vec{D}}$, $\vec{A}$ by this Maxwellian R, we have the equation

$$\nabla\cdot(R\vec{\vec{D}}^{M}\cdot\nabla Z) - \nu RZ = 0 \ . \tag{3.34}$$

Now we write this equation in spherical coordinates (v_1,θ_1,ψ),

$$\left(\frac{1}{v_1^2}\right)\frac{\partial}{\partial v_1}\left\{v_1^2 RD_{\parallel}^{M}\frac{\partial Z}{\partial v_1}\right\} + \left(\frac{1}{v_1^2\sin\theta_1}\right)\frac{\partial}{\partial\theta_1}\left\{\sin\theta_1 RD_{\perp}^{M}\frac{\partial Z}{\partial\theta_1}\right\} \tag{3.35}$$

$$-\nu RZ = 0 \ .$$

The superscript M denotes the Maxwellian version. Since, in the vicinity of the boundary, the unit-vector $\hat{e}_\theta$ is approximately in the direction of $\nabla\eta$ (the normal direction of the boundary surface), and $Z(\eta)$ is only a function of η, we have

$$\left(\frac{1}{v_1}\right)\frac{\partial Z}{\partial\theta_1} >> \frac{\partial Z}{\partial v_1} \ . \tag{3.36}$$

We ignore the first term in Eq. (3.35) to get

$$(1/v_1^2 \sin\theta_1) \frac{d}{d\theta_1} \{\sin\theta_1 R D_\perp^M (\frac{dZ}{d\theta_1})\} - \nu RZ = 0 \qquad (3.37)$$

or

$$\frac{d^2Z}{d\theta_1^2} + \cot\theta_1 (\frac{dZ}{d\theta_1}) - (\frac{\nu v_1^2}{D_\perp^M}) Z = 0 \ . \qquad (3.38)$$

In order to obtain an analytical solution for this equation, we use the basic philosophy again. Let us concentrate on the most important part of the trapping process: the region close to the tip of the boundary, where cot $\theta_1 \sim 0$. Therefore

$$d^2Z/d\theta_1^2 - (\nu v_1^2/D_\perp^M) Z = 0 \ . \qquad (3.39)$$

It has a very simple solution:

$$Z = C_1 \exp(-K\theta_1) + C_2 \exp(+K\theta_1) \ . \qquad (3.40)$$

Here, $K = (\nu v_1^2/D_\perp^M)^{1/2}$. In fact we need only the decaying solution; hence $C_2 = 0$. C_1 is fixed by the boundary condition

$$Z(\theta_{1b}) = 1 \ . \qquad (3.41)$$

Hence

$$Z(\theta_1) = \exp(-K(\theta_1 - \theta_{1b})) \ . \qquad (3.42)$$

Now we introduce the second term in Eq. (3.38); we have an approximate solution

$$Z(\theta_1) = \exp\{-K(\theta_1 - \theta_{1b})(1 - 1/2\ (\theta_1 - \theta_{1b})\ \cot\ \theta_{1b})\}\ . \quad (3.43)$$

This is an exact solution of the equation when $\theta_1 = \theta_{1b}$, so we use it as an approximate solution in the vicinity of the boundary. Therefore, the η coordinate in the vicinity of the boundary is defined as

$$\eta = K(\theta_1 - \theta_{1b})\{1 - 1/2\ (\theta_1 - \theta_{1b})\ \cot\ \theta_{1b}\} \quad (3.44)$$

and the trial function for $Z(\eta)$ may be selected as

$$Z(\eta) = \exp(-a\eta)\ . \quad (3.45)$$

Here, a is a variational parameter, which will be determined by the variational principle. It is noted that $\eta = 0$ on the boundary, and this trial function $Z(\eta)$ satisfies the boundary condition $Z(0) = 1$.

3.5 The Solution of the Variational Problem

Substituting the trial function (3.45) into the functional (3.28), we have

$$L(Z) = \int_0^{\bar{\eta}} d\eta\ \{(a^2 p(\eta) + q_0(\eta))\ \exp(-2a\eta)\} \quad (3.46)$$

and

$$\frac{\partial L}{\partial a} = \int_0^{\bar{\eta}} d\eta\ 2\{(1 - \eta a)a\ p(\eta) - \eta q_0(\eta)\}\ \exp(-2a\eta)\ . \quad (3.47)$$

Since there is an exponential factor $\exp(-2a\eta)$ in the integrand, we may expand $p(\eta)$ and $q_0(\eta)$ around the point $\eta = 0$,

$$\frac{\partial L}{\partial a} = 2 \int_0^{\bar{\eta}} d\eta \{(1 - \eta a)a (p(0) + \eta dp/d\eta|_0) - \eta(q_0(0) + \eta\, dq_0/d\eta|_0)\} \exp(-2a\eta) . \tag{3.48}$$

Using the formula

$$\int_0^{\infty} dx\, x^m \exp(-ax) = m!/a^{(m+1)} \tag{3.49}$$

we have

$$\frac{\partial L}{\partial a} = 2\{p(0)/4 + q_0(0)/(4a^2) - dq_0/d\eta|_{\eta=0} (1/(4a^3))\} . \tag{3.50}$$

The variational principle $\partial L/\partial a = 0$ then gives

$$p(0) - q_0(0)/a^2 - (1/a^3)\, dq_0/d\eta|_{\eta=0} = 0 . \tag{3.51}$$

In fact we can prove that $dq_0/d\eta|_{\eta=0} \approx 0$ (see Appendix II). Thus we have the solution

$$a = \sqrt{q_0(0)/p(0)} . \tag{3.52}$$

3.6 Macro-Balance Equation

Although we have found the solution for the variational parameter, a, we are not able to calculate it yet, since the $\ddot{D}$ tensor in

the p(n) expression depends on the total density, N_b, which is unknown. One more equation is needed. Fortunately, the macro-balance equation provides what we need. Since the pumping rate, ν, is assumed to be constant in the velocity space, the trapping current may be written as

$$J_t = \nu(N_b - N_p) \ . \tag{3.53}$$

Combining Eq. (3.53) with (3.31), we have

$$2p(0)a = \nu(N_b - N_p) \ . \tag{3.54}$$

Using the result of the variational calculation, Eq. (3.52), we have

$$2\sqrt{q_o(0)p(0)} = \nu(N_b - N_p) \ . \tag{3.55}$$

From Eq. (3.19), p(0) is dependent on the total density, N_b, through the diffusion tensor $\vec{\vec{D}}$. Under the single sphere approximation, $\vec{\vec{D}}$ can be written as

$$\vec{\vec{D}}(v) = (2\pi e^4 \frac{\ln \Lambda}{m^2})(\frac{N_b}{2})(\frac{1}{C_o}) \nabla\nabla \int_o^\infty R(v_1)|\vec{v} - \vec{v}_1| \ 4\pi v_1^2 \ dv_1 \ . \tag{3.56}$$

Here C_o is the normalization constant

$$C_o = \int_o^\infty R(v_1) \ 4\pi v_1^2 \ dv_1 \ . \tag{3.57}$$

Now $p(0)$ is proportional to the total density, N_b. Extracting N_b from $p(0)$, we have a quadratic equation for $\sqrt{N_b}$:

$$\nu N_b - 2\sqrt{(p(0)/N_b)q_o(0)}\ \sqrt{N_b} - \nu N_p = 0 \ . \tag{3.58}$$

In the analysis of thermal barriers, it is customary to define a pumping factor, g_b, by

$$g_b = N_b/N_p \ . \tag{3.59}$$

Then, the solution for g_b is

$$g_b = 1 + \alpha(1 + \sqrt{(1 + 2/\alpha)}) \ , \tag{3.60}$$

where

$$\alpha = N_p \hat{q}_o(0)\hat{p}(0)/\nu \ , \tag{3.61}$$

$$\hat{q}_o(0) = q_o(0)/(\nu N_p) \ , \tag{3.62}$$

$$\hat{p}(0) = p(0)/((N_b/2)N_p) \ . \tag{3.63}$$

Once we know g_b, the calculation of the trapping current is straightforward:

$$J_t = \nu N_p(g_b - 1) = \nu N_p \alpha(1 + \sqrt{(1 + 2/\alpha)}) \ . \tag{3.64}$$

4. PRIMARY RESULTS

4.1 Computational Formulae

In order to summarize the analysis so far, we list all the necessary expressions for the calculation of the trapping rate in a thermal barrier.

$$J_t = \nu N_p (g_b - 1) \tag{4.1}$$

$$g_b = 1 + \alpha\left(1 + \sqrt{(1 + 2/\alpha)}\right) \tag{4.2}$$

$$\alpha = N_p \hat{q}_o(0)\ \hat{p}(0)/\nu \tag{4.3}$$

$$\hat{q}_o(0) = 2\pi \int_o^\infty dv_1\ J(v_1,0)\ \hat{R}(v_1) \tag{4.4}$$

$$\hat{R}(v_1) = R(v_1)/N_p \tag{4.5}$$

$$R(v_1) = G \exp\{-(v_1/v_t)^2 - 2(v_1/v_t)(v_{\phi b}/v_t)\cos\theta_{1b}\} \tag{4.6}$$

$$G = (N_p/H)(1/(\sqrt{\pi}\ v_t))^3 \tag{4.7}$$

$$v_t = \sqrt{(2T_p/m)} \tag{4.8}$$

$$H = \exp(y)\ \mathrm{erfc}(\sqrt{y}) - \sqrt{(1/z)}\ \exp(zy)\ \mathrm{erfc}(\sqrt{(zy)}) \tag{4.9}$$

$$y = \phi_b/T_p \tag{4.10}$$

$$z = R_b/(R_b - 1) \tag{4.11}$$

$$v_{\phi b} = \sqrt{(2\phi_b/m)} \tag{4.12}$$

$$\cos\theta_{1b} = (1/R_b)\{-(v_{\phi b}/v_1) + \sqrt{(v_{\phi b}/v_1)^2 + R_b(R_b - 1)}\} \tag{4.13}$$

$$\hat{p}(0) = 2\pi \int_0^\infty dv_1 \frac{J(v_1,0)\ \hat{R}(v_1)}{(0.5\ N_b)} \{D_{\parallel}(\frac{\partial n}{\partial v_1})^2 + D_{\perp}((\frac{1}{v_1})(\frac{\partial n}{\partial \theta_1}))^2\} \tag{4.14}$$

$$J(v_1, n) = v_1^2 \sin\theta_1/(\partial n/\partial\theta_1) \tag{4.15}$$

$$\frac{D_{\parallel}}{0.5\ N_b} = (\frac{2\pi e^4\ \ln\ \Lambda}{m^2})(\frac{1}{v_1})\{\int_0^{v_1} dv_1' (\frac{4\pi v_1'^2}{C_o})\ R(v_1')\ \frac{2}{3}\ (\frac{v_1'}{v_1})^2 + \int_{v_1}^\infty dv_1' (\frac{4\pi v_1'^2}{C_o})\ R(v_1')\ \frac{2}{3}\ (\frac{v_1}{v_1'})\} \tag{4.16}$$

$$\frac{D_{\perp}}{0.5\ N_b} = (\frac{2\pi e^4\ \ln\ \Lambda}{m^2})(\frac{1}{v_1})\{\int_0^{v_1} dv_1' (\frac{4\pi v_1'^2}{C_o})\ R(v_1')\ (1 - (\frac{1}{3})(\frac{v_1'}{v_1})^2) + \int_{v_1}^\infty dv_1' (\frac{4\pi v_1'^2}{C_o})\ R(v_1')\ \frac{2}{3}\ (\frac{v_1}{v_1'})\} \tag{4.17}$$

$$C_o = \int_o^\infty 4\pi v_1^2 \, dv_1 \, R(v_1) \tag{4.18}$$

$$\left.\frac{\partial \eta}{\partial v_1}\right|_{\eta=0} = \frac{K \cot\theta_{1b}}{\left(1 + \left(\frac{v_1}{v_{\phi b}}\right) R_b \cos\theta_{1b}\right)}$$

$$K = \sqrt{(\nu \, v_1^2 / D_\perp^M)} \tag{4.19}$$

$$\partial\eta/\partial\theta_1\big|_{\eta=0} = K$$

Here $D_\perp^M$ in (4.19) is the center shifted Maxwellian version of the diffusion tensor with the density $(N_p/2)$, i.e.

$$D_\perp^M = \left(\frac{2\pi e^4 \ln \Lambda}{m^2}\right)\left(\frac{N_p}{2}\right)\left(\frac{1}{v_1}\right)\left\{\phi(x) - \frac{1}{2x^2}\left(\phi(x) - x\left(\frac{d\phi}{dx}\right)\right)\right\} \tag{4.20}$$

where
$$\phi(x) = (2/\sqrt{\pi}) \int_o^x \exp(-s^2) \, ds \, . \tag{4.21}$$

$$x = v_1/v_t \, . \tag{4.22}$$

The Coulomb logarithm is taken from the form used by Futch and LoDestro [4],

$$\ln \Lambda = 34.9 - 0.5 \ln \left(N/(E_{av} T_e)\right) \, , \tag{4.23}$$

where N is the total density, which is approximated by $3N_p$ in our calculation, E_{av} is the average ion energy in the barrier, which is approximated by $(T_p + \phi_b)$ in our calculation; T_e is approximated by the passing ion temperature T_p. Because these approximations are inside the logarithm, we do not expect any significant error from them.

Although the foregoing formulae look complicated, they are calculable and much simpler than the direct numerical calculation of the Fokker-Planck equation. Usually, the numerical Fokker-Planck code takes 10~20 minutes on the CRAY machine for each run, while our calculation takes only 0.1 second, which is mainly spent on the integrations of $q_0(0)$ and $p(0)$. If it is possible to calculate the integrals in $q_0(0)$ and $p(0)$ analytically, the trapping current in the thermal barrier can be done on a pocket calculator.

4.2 Comparison with Numerical Fokker-Planck Code Results

Futch and LoDestro did a series of numerical Fokker-Planck calculations for the thermal barrier trapping current. These calculations give us a good base for testing our two sphere model and the approximations used in this model. When the variables N_p, T_p, R_b, ϕ_b and ν are used as input, the pumping factor g_b is the output. The comparison with Futch and LoDestro's code calculation is shown in Tables I and II. The agreement is fairly good. For the low mirror ratio cases (Table I), the relative error is generally less than 5%. For the high mirror ratio cases (Table II), the relative error is less than 10%. Considering that there is a numerical error due to

TABLE I. LOW MIRROR RATIO CASE

(R_b = 2, ϕ_b = 40 keV, T_e = 15 keV)

Input Data			g_b		Deviation
N_p	T_p	ν	Numerical*	Variational	
$10^{11}/cm^3$	keV	sec^{-1}			
1.1	15.0	0.25	3.46	3.32	-4%
1.1	15.0	0.50	2.31	2.39	3%
1.1	15.0	1.0	1.80	1.87	4%
1.1	15.0	2.0	1.48	1.56	5%
0.55	15.0	0.25	2.33	2.41	3%
1.1	10.0	0.50	3.62	3.68	2%
1.1	10.0	1.0	2.46	2.59	5%
1.1	10.0	2.0	1.90	1.98	4%
0.55	10.0	0.25	3.66	3.71	1%
2.2	10.0	2.0	2.45	2.57	5%

* Futch and LoDestro [4] (1982)

TABLE II. HIGH MIRROR RATIO CASE

(R_b = 20, ϕ_b = 1.0 keV, T_e = 0.4 keV)

Input Data			g_b		Deviation
N_p	T_p	ν	Numerical*	Variational	
$10^{11}/cm^3$	keV	10^3/sec			
8.9	1/3	2	4.76	4.25	-10%
8.9	1/3	4	2.90	2.90	0%
8.9	1/3	8	2.12	2.16	2%
8.9	0.2	4	5.0	4.57	-9%
8.9	0.4	4	2.54	2.52	-1%
8.9	0.5	4	2.22	2.18	-2%
17.8	1/3	4	4.68	4.21	-10%
4.45	0.2	4	3.06	3.10	1%
17.8	0.4	4	3.79	3.52	7%
4.45	0.4	4	1.94	1.96	1%
17.8	0.5	4	3.10	2.91	-6%

* Futch and LoDestro [4] (1982)

the finite grid size (in the endloss case the grid error is about 7% [7]), we think this agreement is fairly good.

The Futch and LoDestro calculation is non-linear and calculates the Rosenbluth potentials due to the real passing particle distribution and the instantaneous real trapped particle distribution function (including both groups of the particles with plus and minus sings of $v_{\parallel}$). They start from a pure passing particle case; then the trapping process evolves to give more and more trapped particles until it reaches an equilibrium. Our analytical calculation, using the linearized equations, directly calculates the equilibrium state. In this analytical calculation the interaction between the two groups of particles which are moving in opposite directions is neglected. The anisotropic field particle distribution function is approximated by an isotropic sphere. It seems that these approximations are reasonable.

4.3 Discussion

The variational method gives us a powerful method to deal with complicated geometry in velocity space. Although our trial function may not fit the real trapped particle distribution function very well, the resultant error in the trapping current is smaller than the error in the distribution function. Since the trapping current is related to the functional in Eq. (3.31), and the functional is a bilinear form of the function $Z(\eta)$ and $dZ(\eta)/d\eta$, any error in $Z(\eta)$ will result in a second order error in J_t, and therefore in g_b. This effect can also be seen through the analytical expression for g_b.

Since

$$g_b = 1 + \alpha \left(1 + \sqrt{(1 + 2/\alpha)}\right) , \tag{4.24}$$

the error in α will lead to an error in g_b. But the latter is smaller than the former, because the factor $2/\alpha$ decreases while the factor α increases in Eq. (4.24). In fact, we have

$$\frac{\Delta g_b}{g_b} = \left(\frac{\Delta\alpha}{\alpha}\right) \sqrt{(\alpha/(\alpha + 2))} . \tag{4.25}$$

For the range of g_b = 1~5, α is in the range of 0~1.6. Thus we always have

$$\Delta g_b/g_b < (\Delta\alpha/\alpha) . \tag{4.26}$$

Although the accuracy in α is affected by the approximation in our model, the resultant g_b has better accuracy. This is one of the merits of the variational method.

In our calculation, the passing particle density is an input; the total barrier density is an output as a result of the self-consistent calculation. The alternative is to use the total barrier density as the input [18], and calculate the trapping current, J_t, as an output. These two ways are not equivalent; using N_p as input gives a more strict test of the model. When N_p is an input, we have

$$J_t = \nu(N_b - N_p) = \nu N_p(g_b - 1) \ . \tag{4.27}$$

Any error in g_b would produce an error in J_t:

$$\Delta J_t = \nu N_p \Delta g_b \tag{4.28}$$

or
$$(\Delta J_t/J_t)_{N_p\text{input}} = \Delta g_b/(g_b - 1) \ . \tag{4.29}$$

In contrast, when N_b is an input, we have

$$J_t = \nu N_b(1 - 1/g_b) \ ; \tag{4.30}$$

then,
$$\Delta J_t = \nu N_b \Delta g_b/g_b^2 \ , \tag{4.31}$$

$$\left(\frac{\Delta J_t}{J_t}\right)_{N_b\text{input}} = \left(\frac{\Delta g_b}{g_b}\right)\left(\frac{1}{g_b - 1}\right)$$

$$= \frac{1}{g_b}\left(\frac{\Delta J_t}{J_t}\right)_{N_p\text{input}} \ll \left(\frac{\Delta J_t}{J_t}\right)_{N_p\text{input}} \ . \tag{4.32}$$

If we want to test the different models, it is better to compare g_b with the numerical code calculation. Otherwise, the different inputs (N_p or N_b) may affect the comparison in the trapping current J_t. One may see that if $g_b \sim 5$, $(\Delta J_t/J_t)_{N_b\text{input}} \sim 1/4\ (\Delta g_b/g_b)$. Even if the model predicts g_b with an accuracy of only 50%, the accuracy in J_t will not show it.

From the physical point of view, N_b input gives the diffusion tensor $\vec{\vec{D}}$ immediately; the calculation then determines the gradient of the distribution function at the trapped-passing boundary. However, if N_p is input data, the diffusion tensor $\vec{\vec{D}}$ and the gradient of the distribution function should both be obtained self-consistently. Apparently, the latter case requires a better model.

5. ANALYTICAL EXPRESSIONS FOR THE PUMPING FACTOR

5.1 Analytical Expression for g_b ($R_b \gtrsim 1$)

The comparison of the variational calculation with the Fokker-Planck code results, shown in Chapter 4, confirms our two group approximation and two sphere model; in addition, it shows that our trial function is a good approximation. However, the expressions from (4.1) to (4.23) in Chapter 4 are too complicated for a fast calculation of the trapping current. Particularly, the double integration involved in $\hat{p}(0)$ and the integration involved in $\hat{q}_o(0)$ prevent us from being able to obtain a result with only a pocket calculator. We would like to make some approximations to simplify the results further.

The first approximation is to drop $D_{\parallel}$ compared with $D_{\perp}$. Since $D_{\parallel}$ decreases much faster than $D_{\perp}$ when v_1 increases and $\vec{v}_1$ becomes tangential to the trapped-passing boundary when v_1 is small, the contribution to $\hat{p}(0)$ from the $D_{\parallel}\,(\frac{\partial n}{\partial v_1})^2$ term is always suppressed.

The second approximation is that we can use an effective Maxwellian distribution to replace $R(v_1)$ when the mirror ratio R_b is low ($R_b \gtrsim 1$). Since the exponential factor $\exp(-(v_1/v_t)^2)$ causes the most important contribution to come from the $v_1 < v_t$ region, then for $R_b \gtrsim 1$,

$$\cos\theta_{1b} \approx \frac{1}{R_b}\left\{-\left(\frac{v_{\phi b}}{v_1}\right) + \left(\frac{v_{\phi b}}{v_1}\right)\left[1 + \frac{R_b(R_b - 1)}{2(v_{\phi b}/v_1)^2}\right]\right\} = \frac{v_1}{2}\,\frac{(R_b - 1)}{v_{\phi b}}\,. \qquad (5.1)$$

Hence, $$R(v_1) = G \exp\{-(\frac{v_1}{v_t})^2 - 2(\frac{v_1}{v_t})(\frac{v_{\phi b}}{v_t})\frac{v_1}{2}\frac{(R_b - 1)}{v_{\phi b}}\}$$

$$= G \exp\{-R_b(\frac{v_1}{v_t})^2\} . \qquad (5.2)$$

This is a Maxwellian distribution function with an effective temperature of T_p/R_b. For a Maxwellian distribution function, the integration in $D_\perp$ (Eq. (4.18)) can be done analytically. Therefore

$$\frac{D_\perp}{0.5\ N_b} = \frac{2\pi e^4\ \ln\ \Lambda}{m^2}\frac{1}{v_1}\{\phi(x_1) - \frac{1}{2x_1^2}[\phi(x_1) - x_1\frac{d\phi}{dx_1}]\} . \qquad (5.3)$$

Here $\phi(x_1)$ is the error function, and x_1 is defined as

$$x_1 = \frac{\sqrt{R_b}\ v_1}{v_t} . \qquad (5.4)$$

The third approximation is to take the low velocity limit ($v_1 \to 0$) for $D_\perp$ and $D_\perp^M$. Since both $D_\perp$ and $D_\perp^M$ are under the integration with an exponential factor $\exp(-R_b(v_1/v_t)^2)$, the dominant contribution comes from the small v_1 part. Hence

$$\frac{D_\perp}{0.5\ N_b} \to \frac{2\pi e^4\ \ln\ \Lambda}{m^2}\frac{1}{v_1}\frac{4}{3\sqrt{\pi}}\frac{v_1}{(1/\sqrt{R_b})\ v_t}$$

$$= \frac{2\pi e^4\ \ln\ \Lambda}{m^2}\frac{4}{3\sqrt{\pi}}\sqrt{R_b}\frac{1}{v_t} \qquad (5.5)$$

$$D_\perp^M \to \frac{2\pi e^4\ \ln\ \Lambda}{m^2}\frac{N_p/2}{v_1}\frac{4}{3\sqrt{\pi}}\frac{v_1}{v_t} = \text{constant} . \qquad (5.6)$$

Therefore,

$$p(0) = 2\pi(0.5\ N_b) \int_o^\infty dv_1\ J(v_1,0)\ G \exp\left[-R_b\ (\frac{v_1}{v_t})^2\right] \frac{2\pi e^4\ \ln\ \Lambda}{m^2} \frac{4}{3\sqrt{\pi}} \sqrt{R_b}$$

$$\times \frac{1}{v_t}\ (\frac{1}{v_1} \frac{\partial \eta}{\partial \theta_1})^2$$

$$= 2\pi\ G \frac{\Gamma}{2} \frac{N_b}{2} \frac{4}{3\sqrt{\pi}} \sqrt{R_b} \frac{1}{v_t} \int_o^\infty dv_1\ v_1^2\ \sin\theta_{1b} \frac{1}{\left|\frac{\partial \eta}{\partial \theta}\right|} \exp\left[-R_b\ (\frac{v_1}{v_t})^2\right]$$

$$\times\ (\frac{1}{v_1} \frac{\partial \eta}{\partial \theta_1})^2 \qquad (5.7)$$

$$= 2\pi\ G \frac{\Gamma}{2} \frac{N_b}{2} \frac{4}{3\sqrt{\pi}} \sqrt{R_b} \frac{1}{v_t} \int_o^\infty dv_1\ \sin\theta_{1b}\ (\frac{\partial \eta}{\partial \theta_1}) e^{-R_b(v_1/v_t)^2}$$

$$= 2\pi\ G \frac{\Gamma}{2} \frac{N_b}{2} \frac{4}{3\sqrt{\pi}} \sqrt{R_b} \frac{1}{v_t} \sqrt{\frac{\nu}{D_\perp^M}} \int_o^\infty dv_1\ \sin\theta_{1b}\ v_1 e^{-R_b(v_1/v_t)^2} .$$

The fourth approximation is to assume $\sin\theta_{1b} \approx 1$ in the integrand of Eq. (5.7). Hence,

$$p(0) = 2\pi\ G \frac{\Gamma}{2} \frac{N_b}{2} \frac{4}{3\sqrt{\pi}} \sqrt{R_b} \frac{1}{v_t} \sqrt{\frac{\nu}{D_\perp^M}} \int_o^\infty dv_1\ v_1 e^{-R_b(v_1/v_t)^2}$$

$$(5.8)$$

$$= 2\pi\ G \frac{\Gamma}{2} \frac{N_b}{2} \frac{4}{3\sqrt{\pi}} \sqrt{R_b} \frac{1}{v_t} \sqrt{\frac{\nu}{D_\perp^M}} \frac{v_t^2}{2R_b} .$$

Using the same approach, we have

$$q_o(0) = 2\pi \int_o^\infty dv_1\, v_1^2 \sin\theta_{1b} \frac{\nu}{\left|\frac{\partial\eta}{\partial\theta}\right|} G \exp\left[-R_b\left(\frac{v_1}{v_t}\right)^2\right]$$

$$\approx 2\pi G \frac{\nu}{\sqrt{\nu/D_\perp^M}} \int_o^\infty dv_1\, v_1 \exp\left[-R_b\left(\frac{v_1}{v_t}\right)^2\right] = 2\pi G \sqrt{\frac{D_\perp^M}{\nu}} \left(\frac{v_t^2}{2R_b}\right) \nu \,. \tag{5.9}$$

Hence

$$\alpha = \frac{q_o(0)\, p(0)}{\nu^2 N_p (0.5\, N_b)}$$

$$= (2\pi G)^2 \frac{\Gamma}{2} \frac{4}{3\sqrt{\pi}} \left(\frac{v_t^2}{2R_b}\right)^2 \frac{\sqrt{R_b}}{v_t} \frac{\nu}{\nu^2 N_p}$$

$$= \frac{2}{3\pi} \frac{\nu_c}{\nu} \frac{N_c}{N_p} \frac{1}{\sqrt{\pi}} \left(\frac{1}{\sqrt{R_b}}\right)^3 \,. \tag{5.10}$$

Here, the collision frequency ν_c corresponds to the thermal velocity v_t and central cell density N_c, i.e.

$$\nu_c \equiv \frac{4\pi e^4 \ln \Lambda}{m^2} \frac{1}{v_t^3} \frac{N_p}{H} \tag{5.11}$$

where H is given in Eq. (4.9). Table III shows the results of the calculation using Eq. (5.10) for the same cases considered in Table I. The deviation from Futch and LoDestro's calculation is less than 6%. This agreement encourages us to go further to get a general analytical expression for α.

TABLE III. LOW MIRROR RATIO CASE

(R_b = 2, ϕ_b = 40 keV, T_e = 15 keV)

Input Data			g_b		Deviation
N_p	T_p	ν	Numerical*	Variational	
$10^{11}/cm^3$	keV	sec^{-1}			
1.1	15.0	0.25	3.46	3.32	-4%
1.1	15.0	0.50	2.31	2.39	3%
1.1	15.0	1.0	1.80	1.87	4%
1.1	15.0	2.0	1.48	1.56	5%
0.55	15.0	0.25	2.33	2.40	3%
1.1	10.0	0.50	3.62	3.71	2%
1.1	10.0	1.0	2.46	2.61	6%
1.1	10.0	2.0	1.90	1.99	5%
0.55	10.0	0.25	3.66	3.74	2%
2.2	10.0	2.0	2.45	2.59	6%

* Futch and LoDestro [4] (1982)

5.2 Analytical Expression for g_b (R_b = 2-20)

We now consider the case of arbitrary mirror ratio. Let us first check the four approximations made in Section 5.1. $D_{\parallel}$ is still less than $D_{\perp}$ in the general case, but $R(v_1)$ is no longer a Maxwellian distribution. Since the range $R_b >> 1$ is now included, $\cos\theta_{1b}$ may no longer be expressed by Eq. (5.1), and therefore Eq. (5.2) is no longer valid. Consequently, the third approximation should be corrected, and $\sin\theta_{1b} \sim 1$ is no longer a good approximation as well.

When $R(v_1)$ is not Maxwellian, the first problem is to find a way to avoid the double integration in p(0). Since

$$\frac{D_{\perp}(v_1)}{0.5\ N_b} = \frac{2\pi e^4\ \ln\Lambda}{m^2}\frac{1}{v_1}\frac{1}{C_o}\left\{\int_o^{v_1} dv_1'\ 4\pi v_1'^2\ R(v_1')\left[1 - \frac{1}{3}\left(\frac{v_1'}{v_1}\right)^2\right]\right. \tag{5.12}$$
$$\left. + \int_{v_1}^{\infty} dv_1'\ 4\pi v_1'^2\ R(v_1')\ \frac{2}{3}\left(\frac{v_1}{v_1'}\right)\right\},$$

we may write

$$\frac{D_{\perp}(v_1)}{0.5\ N_b} = \frac{\Gamma}{2}\frac{1}{v_1}\frac{1}{C_o}\left\{\int_o^{v_1} dv_1'\ 4\pi v_1'^2\ R(v_1')\left[1 - \frac{1}{3}\left(\frac{v_1'}{v_1}\right)^2 - \frac{2}{3}\left(\frac{v_1}{v_1'}\right)\right]\right.$$
$$\left. + \int_o^{\infty} dv_1'\ 4\pi v_1'^2\ R(v_1')\ \frac{2}{3}\left(\frac{v_1}{v_1'}\right)\right\} \tag{5.13}$$
$$= \frac{\Gamma}{2}\frac{1}{v_1}\frac{1}{C_o}\left\{O(v_1^3) + \int_o^{\infty} dv_1'\ 4\pi v_1'^2\ R(v_1')\ \frac{2}{3}\left(\frac{v_1}{v_1'}\right)\right\}.$$

The first term inside the brackets decreases with v_1 much faster than

the second term. Because this expression for $D_\perp(v_1)$ is used to calculate the integration in the expression for $\hat{p}(0)$ (Eq. (4.14)), the $\hat{R}(v_1)$ in the integrand makes the contribution from the small v_1 part dominant. Thus we can neglect the first term in Eq. (5.13). Then the double integration in (4.14) becomes the product of two single integrations. Therefore,

$$\alpha = \frac{N_p}{\nu}\left[2\pi \int_0^\infty dv_1\, J(v_1,0)\, \hat{R}(v_1)\right]\left[2\pi \int_0^\infty dv_1\, J(v_1,0)\, \hat{R}(v_1)\right.$$

$$\left. \times \left\{\frac{\Gamma}{2}\frac{1}{v_1}\frac{1}{C_o}\int_o^\infty dv_1'\, 4\pi v_1'^2\, R(v_1')\, \frac{2}{3}\,(\frac{v_1}{v_1'})(\frac{1}{v_1}\frac{\partial \eta}{\partial \theta_1})^2\right\}\right] \qquad (5.14)$$

$$= \frac{N_p}{\nu}\,(2\pi\,\frac{G}{N_p})^2\,\frac{\Gamma}{3}\,\frac{\{\int_o^\infty dv_1\, v_1\, \sin\theta_{1b}\, \tilde{R}(v_1)\}^2 \int_o^\infty dv_1'\, v_1'\, \tilde{R}(v_1')}{\int_o^\infty dv_1\, v_1^2\, \tilde{R}(v_1)}\,.$$

Here,
$$\tilde{R}(v_1) \equiv \exp\{-(\frac{v_1}{v_t})^2 - 2(\frac{v_1}{v_t})(\frac{v_{\phi b}}{v_t})\cos\theta_{1b}\}\,. \qquad (5.15)$$

Therefore,

$$\alpha = \frac{1}{3\pi}\,\frac{\nu_c}{\nu}\,\frac{N_c}{N_p}\,\frac{\hat{I}_1^2 \cdot \hat{I}_2}{\hat{I}_3} \qquad (5.16)$$

where:
$$\hat{I}_1 = \int_o^\infty d(\frac{v_1}{v_t})^2\, \sin\theta_{1b}\, \tilde{R}(v_1)\,, \qquad (5.17)$$

$$\hat{I}_2 = \int_o^\infty d(\frac{v_1}{v_t})^2\, \tilde{R}(v_1)\,, \qquad (5.18)$$

$$\hat{I}_3 = \int_0^\infty d\left(\frac{v_1}{v_t}\right)^2 \left(\frac{v_1}{v_t}\right) \tilde{R}(v_1) \ . \tag{5.19}$$

This expression (5.16) is valid for both high and low mirror ratio cases. When $R_b \gtrsim 1$,

$$\tilde{R}(v_1) \to \exp\left\{-R_b \left(\frac{v_1}{v_t}\right)^2\right\} \ , \tag{5.20}$$

and $\sin\theta_{1b} \sim 1$, and we have

$$\hat{I}_1 = \hat{I}_2 = \int_0^\infty dx \ e^{-R_b x} = \frac{1}{R_b} \tag{5.21}$$

$$\hat{I}_3 = \int_0^\infty dx \ \sqrt{x} \ e^{-R_b x} = \frac{\sqrt{\pi}}{2} \left(\frac{1}{R_b}\right)^{3/2} \ . \tag{5.22}$$

Hence,
$$\alpha = \frac{2}{3\pi} \frac{\nu_c}{\nu} \frac{N_c}{N_p} \frac{1}{\sqrt{\pi}} \left(\frac{1}{R_b}\right)^{3/2} \ . \tag{5.23}$$

This is just the same expression as we got in the last section (e.g., (5.10)).

Now our task is to calculate three integrations (5.17)-(5.19) for the general case. Using the two point Laguerre-Gauss quadrature formula (Appendix III), we have

$$\hat{I}_i = Z_1 f_i(\hat{x}_1) + Z_2 f_i(\hat{x}_2) \tag{5.24}$$

Here,

$$Z_1 = \frac{2 + \sqrt{2}}{4\sqrt{2 - \sqrt{2} + \alpha_\ell^2}}$$

$$Z_2 = \frac{2 - \sqrt{2}}{4\sqrt{2 + \sqrt{2} + \alpha_\ell^2}} \tag{5.25}$$

$$\hat{x}_1 = \sqrt{2 - \sqrt{2} + \alpha_\ell^2} - \alpha_\ell$$

$$\hat{x}_2 = \sqrt{2 + \sqrt{2} + \alpha_\ell^2} - \alpha_\ell \tag{5.26}$$

$$f_i(\hat{x}) = \begin{cases} \overline{R}(\hat{x})\ \hat{x}\ \sin\theta_{1b} & i = 1 \\ \overline{R}(\hat{x})\ \hat{x} & i = 2 \\ \overline{R}(\hat{x})\ \hat{x}^2 & i = 3 \end{cases} \tag{5.27}$$

$$\overline{R}(\hat{x}) = \exp\{2\hat{x}[\alpha_\ell + \delta_\ell - \sqrt{\delta_\ell^2 + \alpha_\ell^2}]\} \tag{5.28}$$

$$\delta_\ell = \frac{\phi_b}{T_p}\frac{1}{R_b}\frac{1}{\hat{x}} \tag{5.29}$$

$$\alpha_\ell = \sqrt{\frac{\phi_b}{T_p}\left(1 - \frac{1}{R_b}\right)} \tag{5.30}$$

$$\sqrt{\frac{\phi_b}{T_p}}\cos\theta_{1b} = -\delta_\ell + \sqrt{\delta_\ell^2 + \alpha_\ell^2} \tag{5.31}$$

It should be noticed that $\overline{R}$ in (5.27) is not $\tilde{R}$ in (5.15). In order

to use the two point Laguerre-Gauss quadrature formula in Appendix III, we must extract the $e^{-\beta x^2 - \gamma x}$ factor from the $\tilde{R}(v_1)$ in the correct way. Let $v_1 \to \infty$,

$$\tilde{R}(v_1) \to \exp\{-(\frac{v_1}{v_t})^2 - 2(\frac{v_1}{v_t})(\frac{v_{\phi b}}{v_t})\sqrt{1 - \frac{1}{R_b}}\} . \qquad (5.32)$$

In this way we find that

$$\beta = (\frac{1}{v_t})^2 \qquad (5.33)$$

$$\gamma = 2\frac{v_{\phi b}}{v_t^2}\sqrt{1 - \frac{1}{R_b}} = 2\sqrt{\frac{\phi_b}{T_p}}\sqrt{\beta}\sqrt{1 - \frac{1}{R_b}} \qquad (5.34)$$

and
$$\bar{R}(\hat{x}) = \exp\{2\hat{x}\sqrt{\frac{\phi_b}{T_p}(1 - \frac{1}{R_b})} - 2\hat{x}\sqrt{\frac{\phi_b}{T_p}}\cos\theta_{1b}\}$$
$$= \exp\{2\hat{x}[\alpha_\ell + \delta_\ell - \sqrt{\delta_\ell^2 + \alpha_\ell^2}]\} . \qquad (5.35)$$

Figure 12 shows the result of calculations based on Eqs. (5.16) and (5.24)-(5.31). The deviation from Futch and LoDestro's code result is generally less than 20%. Considering that it covers the range of R_b = 2~20, we think that it is a fairly good approximation. Figure 13 shows a similar plot of the numerical-variational calculation in Section 4 compared with the results of Futch and LoDestro. We see that the additional errors introduced in the approximations used to get an analytical expression for α are not large.

Fig. 12. Comparison between the results from the variational calculation (two point Laguerre-Gauss Quadrature) and Futch and LoDestro's code calculation.

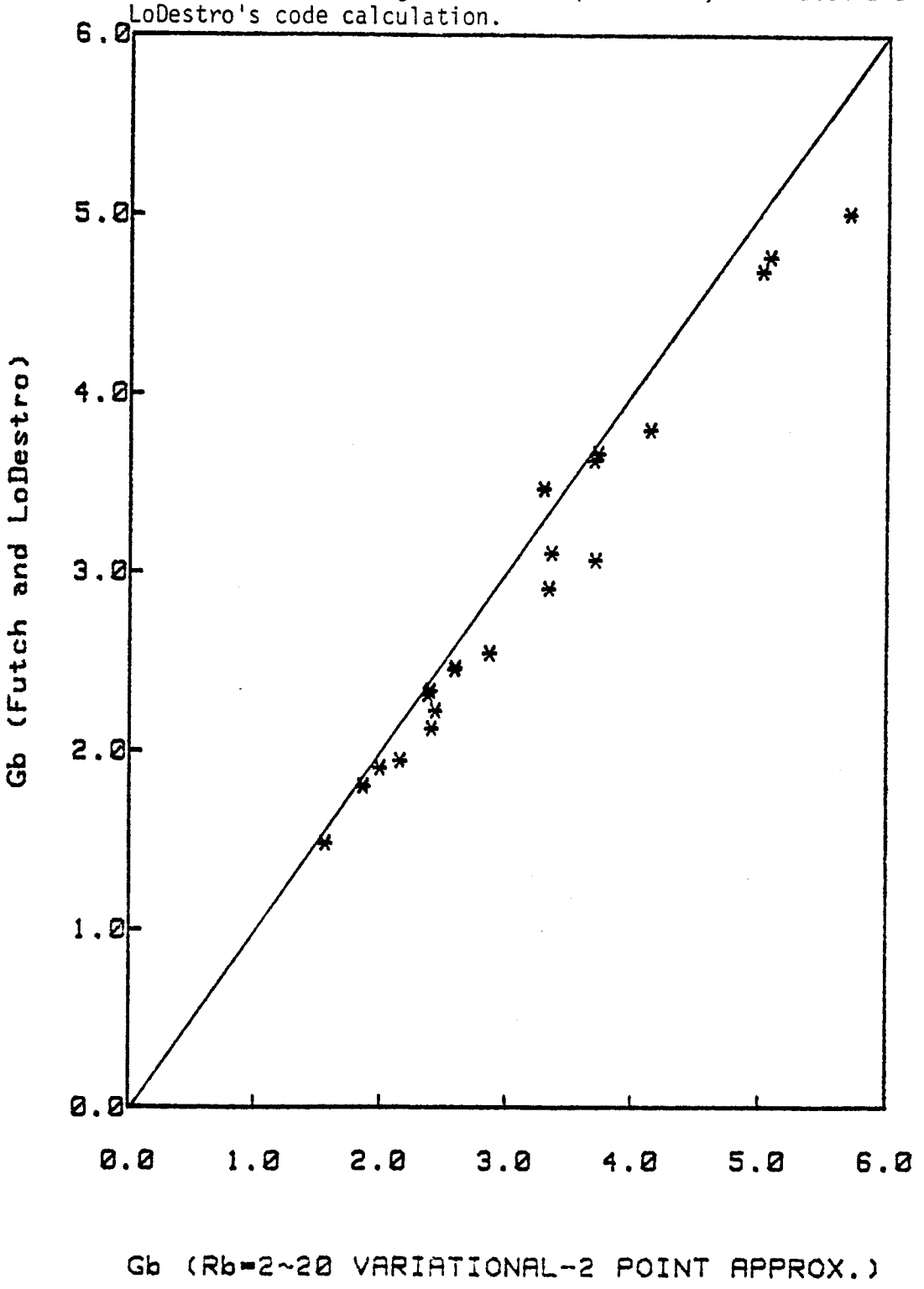

Fig. 13. Comparison between the results from the variational calculation (exact integration) and the Futch and LoDestro's code calculation.

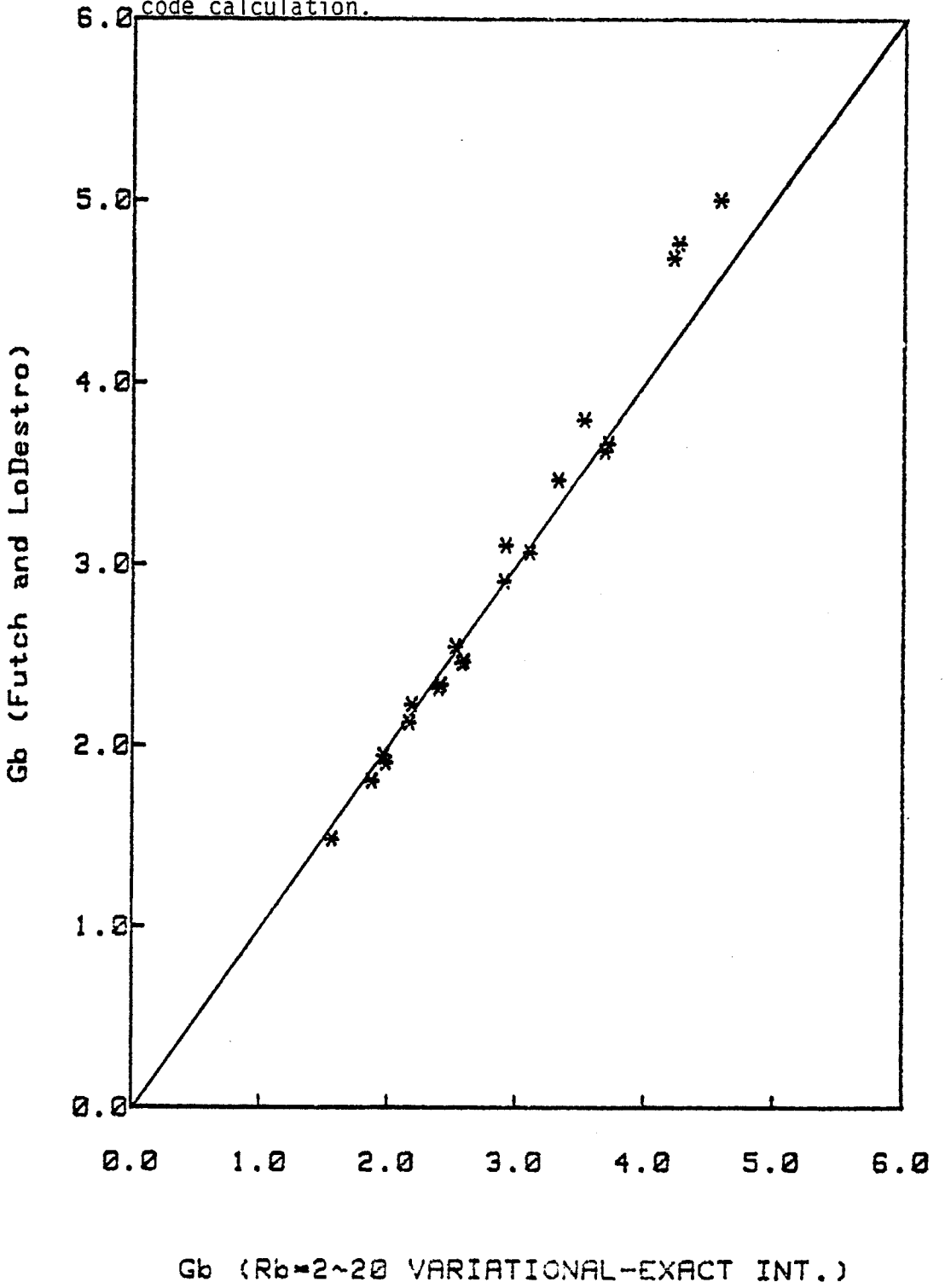

6. SUMMARY

6.1 Physics

The trapping process in the thermal barrier is a collisional process. Three aspects of this collisional process were unclear to us when we started this research: (i) To what extent do collisions between the two groups of counter-streaming particles contribute to the trapping process? (ii) Which part of the trapped passing-boundary surface is essential for the current across the boundary? (iii) Does pitch angle scattering dominate the trapping process or does energy diffusion play an important role in this process? As a result of our research, we can say that: (i) When the barrier is well pumped ($\phi_b/T_p \gtrsim 2$), collisions between the two counter-streaming groups is negligible compared with collisions among the particles moving in the same direction. Because of the velocity dependence of the Rutherford cross-section, the interaction is small when the relative velocity of two particles is large. (ii) The tip of the boundary surface is the most important part for calculating the current across the boundary. Because most of the particles are concentrated in the region around the tip, the particles in the vicinity of the tip experience the strongest scattering and the number of these particles is a big fraction of the total number of the particles in the barrier. Therefore, careful treatment of this part of the boundary is essential for the calculation of the trapping current. (iii) The energy diffusion process is not negligible, since the drag

force between trapped particles and passing particles causes a substantial current across the boundary. This effect may be more important in the non-square well case, where the density is peaked near the magnetic peak. Since the collision rate is proportional to the square of the density, the trapping process near the magnetic peak is essential for the analysis. However, in the region very close to the peak, the local mirror ratio is very small, and consequently, pitch angle scattering in this region (i.e., a change in magnetic moment) may not have a big effect on the trapping current. In contrast, the drag force between trapped particles and passing partices may retard the passing particles and contribute to the trapping process regardless of the local mirror ratio.

Our model has a better treatment of these three aspects, so the agreement with the numerical Fokker-Planck code results is better.

6.2 Mathematics

When Chernin and Rosenbluth started their variational calculation of the Pastukhov problem, their goal was to check the effect of the deformation of the boundary on the endloss. So they changed the shape of the loss-cone boundary widely. Later Catto and Bernstein developed this variational calculation by the contour method for specifying the trial functions. This allowed treating the boundary much better than before. It was not expected that a variational functional could be found for a thermal barrier where the distribution function is non-Maxwellian. In this research we have

found a functional for the thermal barrier case using the two group approximation and two sphere model.

In addition to applying Catto and Bernstein's contour method, we put emphasis on the most important region and used the asymptotic behavior to guess the shape of the contours in velocity space. The application of these two principles led us to an analytical expression for the trapping current in a thermal barrier. Success encourages us to apply it in the Pastukhov problem, the weak pumping case [23] and multiple species pumping case (e.g., D-T mixture). This, however, is left for future work.

A final closed form analytical expression for the trapping current in the well pumped barrier has been obtained. For the barrier mirror ratio from 2 to 20, it deviates from Futch and LoDestro's Fokker-Planck code results [4] with an error of less than 20%. Considering that the Fokker-Planck equation itself has an error of about 5% ($1/\ln \Lambda$) and the finite grid error in the code result is about 7%, we think this is good enough for general purposes in calculating the trapping current. The two point Laguerre-Gauss quadrature formula used in obtaining this closed form analytical expression is a powerful tool for future work.

The computer time necessary for the Fokker-Planck code is 10~20 minutes on the Cray computer for each case, and the computer time for our formulae (4.1)-(4.23) is less than 0.1 sec. Finally the formulae (5.16)-(5.31) are calculable even on a pocket calculator.

APPENDIX I. A GENERALIZED GAUSS' THEOREM

In any coordinate system, we have Gauss' Theorem

$$\iiint d^3v \ \nabla\cdot\vec{C} \equiv \iint d\vec{S}\cdot\vec{C} \ . \tag{I.1}$$

Using the coordinate system (v_1, η, ψ) with the Jacobian J, we obtain

$$\iiint d^3v \ \nabla\cdot\vec{C} = \iiint d\eta dv_1 d\psi \ J\nabla\cdot\vec{C} \ . \tag{I.2}$$

For the vector set $(\nabla v_1, \nabla\eta, \nabla\psi)$ there is a reciprocal vector set $(\frac{\partial\vec{v}}{\partial v_1}, \frac{\partial\vec{v}}{\partial\eta}, \frac{\partial\vec{v}}{\partial\psi})$; therefore

$$\nabla\eta = (\frac{\partial\vec{v}}{\partial\psi}) \times (\frac{\partial\vec{v}}{\partial v_1}) \ / \ [(\frac{\partial\vec{v}}{\partial\psi}) \times (\frac{\partial\vec{v}}{\partial v_1}) \cdot (\frac{\partial\vec{v}}{\partial\eta})] \ . \tag{I.3}$$

However, the Jacobian J can be defined as

$$J = (\frac{\partial\vec{v}}{\partial\psi}) \times (\frac{\partial\vec{v}}{\partial v_1}) \cdot (\frac{\partial\vec{v}}{\partial\eta}) \ . \tag{I.4}$$

Hence,

$$(\frac{\partial\vec{v}}{\partial\psi}) \times (\frac{\partial\vec{v}}{\partial v_1}) = J\nabla\eta \ . \tag{I.5}$$

Since the differential surface element at constant η can be written as

$$d\vec{S} = (\frac{\partial\vec{v}}{\partial\psi}) \times (\frac{\partial\vec{v}}{\partial v_1}) \, d\psi dv_1 \ , \tag{I.6}$$

we have

$$\iint d\vec{S}\cdot\vec{C} = \iint \left(\frac{\partial\vec{v}}{\partial\psi}\right) \times \left(\frac{\partial\vec{v}}{\partial v_1}\right) dv_1 d\psi\cdot\vec{C} = \iint dv_1 d\psi\, J\nabla\eta\cdot\vec{C} \ . \qquad (I.7)$$

Substituting Eqs. (I.2) and (I.7) into Eq. (I.1), we have

$$\iiint d\eta dv_1 d\psi\, J\nabla\cdot\vec{C} = \iint dv_1 d\psi\, J\nabla\eta\cdot\vec{C} \ . \qquad (I.8)$$

Taking the derivative with respect to η on both sides of Eq. (I.8), we have our desired result,

$$\iint dv_1 d\psi\, J\nabla\cdot\vec{C} = \frac{d}{d\eta} \iint dv_1 d\psi\, J\nabla\eta\cdot\vec{C} \ . \qquad (I.9)$$

APPENDIX II. THE CALCULATION OF $\left.\frac{dq_o}{d\eta}\right|_{\eta=0}$

We have

$$q_o(\eta) \equiv 2\pi \int_{v_{min}}^{\infty} dv_1 \; J(v_1,\eta)\nu R(v_1) \; . \tag{II.1}$$

The lower limit of the integration, v_{min}, is not zero when η is non-zero, since v_1 is the distance from the tip of the $\eta = 0$ surface to any point on the η = constant surface. Now

$$\frac{d}{d\eta} q_o(\eta) = -2\pi J(v_{min},\eta) \; \nu R(v_{min}) \cdot \frac{dv_{min}}{d\eta} + 2\pi \int_{v_{min}}^{\infty} dv_1 \; \nu R(v_1) \frac{\partial}{\partial \eta} J(v_1,\eta) \; . \tag{II.2}$$

Since

$$J(v_1,\eta) = v_1^2 \sin\theta_1 \left|\frac{1}{\frac{\partial \eta}{\partial \theta_1}}\right| \tag{II.3}$$

and

$$\theta_1(v_{min},\eta) = \pi$$

we have

$$J(v_{min},\eta) = 0 \; . \tag{II.4}$$

For the second term in Eq. (II.2), we use

$$\frac{\partial}{\partial \eta} J(v_1,\eta) = v_1^2 \frac{\partial}{\partial \eta}\left[\sin\theta_1 \frac{1}{(\frac{\partial \eta}{\partial \theta_1})}\right]$$

$$= v_1^2\left[\cos\theta_1 (\frac{\partial \theta_1}{\partial \eta}) \frac{1}{(\frac{\partial \eta}{\partial \theta_1})} + \sin\theta_1 \frac{(-1)}{(\frac{\partial \eta}{\partial \theta_1})^2} \frac{\partial}{\partial \eta}(\frac{\partial \eta}{\partial \theta_1})\right] . \tag{II.5}$$

However,
$$\frac{\partial}{\partial \eta}(\frac{\partial \eta}{\partial \theta_1}) = (\frac{\partial^2 \eta}{\partial \theta_1^2})(\frac{\partial \theta_1}{\partial \eta}) = \frac{1}{(\frac{\partial \eta}{\partial \theta_1})}(\frac{\partial^2 \eta}{\partial \theta_1^2}) . \tag{II.6}$$

From Eq. (3.44), we have

$$\frac{\partial \eta}{\partial \theta_1} = \sqrt{\frac{w_1^2}{D_\perp^M}}\left[1 - (\cot\theta_{1b})(\theta_1 - \theta_{1b})\right] \tag{II.7}$$

$$\frac{\partial^2 \eta}{\partial \theta_1^2} = -\sqrt{\frac{w_1^2}{D_\perp^M}} \cot\theta_{1b} . \tag{II.8}$$

Hence

$$\frac{\partial}{\partial \eta} J(v_1,\eta) = v_1^2\left[\cos\theta_1 \frac{1}{(\frac{\partial \eta}{\partial \theta_1})^2} - \sin\theta_1 \frac{1}{(\frac{\partial \eta}{\partial \theta_1})^2} \frac{(-\cot\theta_{1b})}{1 - \cot\theta_{1b}(\theta_1 - \theta_{1b})}\right]$$

$$\underset{\theta_1 \to \theta_{1b}}{=} v_1^2 \frac{1}{(\frac{\partial \eta}{\partial \theta_1})^2}\left[\cos\theta_{1b} + \sin\theta_{1b} \cot\theta_{1b}\right] \tag{II.9}$$

$$\to v_1^2 \frac{1}{(\frac{\partial \eta}{\partial \theta_1})^2} 2\cos\theta_{1b} = 2\frac{J(v_1,0) \cot\theta_{1b}}{(\frac{\partial \eta}{\partial \theta_1})} .$$

So
$$\left.\frac{d}{d\eta} q_o(\eta)\right|_{\eta=0} = 2\pi \int_o^\infty dv_1 \, J(v_1,0) \frac{2\cot\theta_{1b}}{\sqrt{\frac{\nu v_1^2}{D_\perp^M}}} \nu R(v_1) \, . \tag{II.10}$$

Since $R(v_1)$ is a dramatically descending function of v_1, only small v_1 contributes to the integration. For small v_1, we have

$$\cot\theta_{1b} \xrightarrow[v_1 \to 0]{} \cos\theta_{1b} \sim \frac{v_1}{2v_{\phi b}} (R_b - 1) \tag{II.11}$$

$$\sqrt{\frac{\nu v_1^2}{D_\perp^M}} \xrightarrow[v_1 \to 0]{} \sqrt{\frac{\nu}{\frac{\Gamma}{2} \frac{N_p}{2} \frac{1}{v_1} \frac{4}{3\sqrt{\pi}} \left(\frac{v_1}{v_t}\right)}} v_1$$

$$\sim \sqrt{\frac{\nu}{\frac{1}{3} \frac{1}{\sqrt{\pi}} \Gamma N_p \frac{1}{v_t^3}}} \left(\frac{v_1}{v_t}\right) \sim \sqrt{\frac{\nu}{\nu_c}} \left(\frac{v_1}{v_t}\right) . \tag{II.12}$$

Here, ν_c is the order of the collision frequency of the passing particles, which is much less than the pumping rate ν in the strong pumping case. Hence,

$$\frac{\cot\theta_{1b}}{\sqrt{\nu v_1^2 / D_\perp^M}} \xrightarrow[v_1 \to 0]{} \sqrt{\frac{\nu_c}{\nu}} \frac{1}{2} \left(\frac{v_t}{v_{\phi b}}\right)(R_b - 1) \ll 1 \, . \tag{II.13}$$

Therefore, $\left.\frac{d}{d\eta} q_o(\eta)\right|_{\eta \to 0}$ is negligible compared to $q_o(\eta \to 0)$.

APPENDIX III. LAGUERRE-GAUSS QUADRATURE FORMULA

In general, an integration with an exponential factor $e^{-\alpha x}$ may be expressed as a Gaussian-Laguerre series, i.e.

$$I_1(x) = \int_0^\infty e^{-\alpha x} f(x)\, dx = \sum_{i=1}^{\infty} H_i\, f(x_i)\ . \qquad \text{(III.1)}$$

Sometimes only two terms of this expansion may give good accuracy [24].

$$I_1(x) = \int_0^\infty e^{-\alpha x} f(x)\, dx = \frac{1}{\alpha}\left[\frac{2+\sqrt{2}}{4} f\left(\frac{2-\sqrt{2}}{\alpha}\right) + \frac{2-\sqrt{2}}{4} f\left(\frac{2+\sqrt{2}}{\alpha}\right)\right] + \frac{f^{iv}(\xi)}{6\alpha^5}\ . \qquad 0 < \xi < \infty \qquad \text{(III.2)}$$

For example, when $f(x) = 1$, the exact value of this integration is $1/\alpha$; this formula (III.2) gives

$$\int_0^\infty e^{-\alpha x}\, 1\, dx = \frac{1}{\alpha}\left[\frac{2+\sqrt{2}}{4} + \frac{2-\sqrt{2}}{4}\right] = \frac{1}{\alpha}\ . \qquad \text{(III.3)}$$

Usually, the two point Gaussian quadrature formula gives a good approximation of the integration as long as $f(x)$ has reasonable behavior (such as a polynomial).

For the case of the integration

$$I_2(x) = \int_0^\infty e^{-\beta x^2 - \gamma x} f(x)\, dx\ , \qquad \text{(III.4)}$$

there is a fast decaying factor $e^{-\beta x^2-\gamma x}$ and one may expand f(x) as a Taylor series around the point x = 0. Then the parabolic cylinder function $D_{-\nu}(x)$ may be used to express this integration [25]:

$$I_2(x) = \int_0^\infty e^{-\beta x^2-\gamma x} \left[f(0) + x \left.\frac{\partial f}{\partial x}\right|_0\right] dx$$

$$= (2\beta)^{-1/2} \Gamma(1) \exp\left(\frac{\gamma^2}{8\beta}\right) D_{-1}\left(\frac{\gamma}{\sqrt{2\beta}}\right) f(0)$$

$$+ (2\beta)^{-1} \Gamma(2) \exp\left(\frac{\gamma^2}{8\beta}\right) D_{-2}\left(\frac{\gamma}{\sqrt{2\beta}}\right) \left.\frac{\partial f}{\partial x}\right|_0 .$$

However, one may simply use the two point Gaussian quadrature formula to avoid the parabolic cylinder function and the derivative of f(x). That is

$$I_2(x) = \int_0^\infty e^{-\beta(x+(\gamma/2\beta))^2+(\gamma^2/4\beta)} f(x)\, dx$$

$$= e^{\gamma^2/4\beta} \int_{\gamma/2\beta}^\infty e^{-\beta S^2} f\left(S - \frac{\gamma}{2\beta}\right) dS$$

$$= e^{\gamma^2/4\beta} \int_{(\gamma/2\beta)^2}^\infty e^{-\beta t} f\left(\sqrt{t} - \frac{\gamma}{2\beta}\right) d\sqrt{t}$$

$$= \int_{(\gamma/2\beta)^2}^\infty e^{-\beta[t-(\gamma/2\beta)^2]} \frac{f\left(\sqrt{t} - \frac{\gamma}{2\beta}\right)}{2\sqrt{t}} dt$$

$$= \int_0^\infty e^{-\beta t'} \frac{f\left(\sqrt{t' + (\gamma/2\beta)^2} - \frac{\gamma}{2\beta}\right)}{2\sqrt{t' + (\gamma/2\beta)^2}}\, dt'$$

$$= \frac{1}{2\beta}\left\{\frac{2+\sqrt{2}}{4} \frac{1}{\sqrt{\frac{2-\sqrt{2}}{\beta} + \left(\frac{\gamma}{2\beta}\right)^2}} f\left(\sqrt{\frac{2-\sqrt{2}}{\beta} + \left(\frac{\gamma}{2\beta}\right)^2} - \frac{\gamma}{2\beta}\right)\right.$$

$$\left. + \frac{2-\sqrt{2}}{4} \frac{1}{\sqrt{\frac{2+\sqrt{2}}{\beta} + \left(\frac{\gamma}{2\beta}\right)^2}} f\left(\sqrt{\frac{2+\sqrt{2}}{\beta} + \left(\frac{\gamma}{2\beta}\right)^2} - \frac{\gamma}{2\beta}\right)\right\} .$$

In our case, $\beta = (1/v_t)^2$; $\gamma = 2(v_{\phi b}/v_t^2)\sqrt{1 - (1/R_b)} = 2\sqrt{\phi_b/T_p}\ \sqrt{\beta}\ \sqrt{1 - (1/R_b)}$; $(\gamma/2\beta) = 2\sqrt{\phi_b/T_p}\ \sqrt{\beta}\ \sqrt{(1 - (1/R_b))}/2\beta = \sqrt{\phi_b/T_p}\ 1/\sqrt{\beta}\ \sqrt{1 - (1/R_b)} \equiv \alpha_\ell v_t$. Here

$$\alpha_\ell \equiv \sqrt{\frac{\phi_b}{T_p}\left(1 - \frac{1}{R_b}\right)} . \qquad \text{(III.5)}$$

Hence,

$$I_2(x) = \frac{v_t}{2}\left\{\frac{2+\sqrt{2}}{4} \frac{1}{\sqrt{2 - \sqrt{2} + \alpha_\ell^2}} f\left[\left(\sqrt{2 - \sqrt{2} + \alpha_\ell^2} - \alpha_\ell\right) v_t\right]\right.$$

$$\left. + \frac{2-\sqrt{2}}{4} \frac{1}{\sqrt{2 + \sqrt{2} + \alpha_\ell^2}} f\left[\left(\sqrt{2 + \sqrt{2} + \alpha_\ell^2} - \alpha_\ell\right) v_t\right]\right\} . \qquad \text{(III.6)}$$

REFERENCES

1. Fowler, T.K. and Logan, B.G., Comments on Plasma Physics and Controlled Fusion 2, 167 (1977). Dimov, G.I., Zakaydakov, V.V., Kishinevskiy, M.Ye., Fizika Plasmy 2, 597 (1976).

2. Baldwin, D.E., Logan, B.G., Phys. Rev. Lett. 43, 1318 (1979).

3. Logan, B.G., private communication (1982).

4. Futch, A.H., LoDestro, L.L., UCRL-87249 (1982).

5. Pastukhov, V.P., Nucl. Fusion 14, 3 (1974).

6. Chernin, D.P., Rosenbluth, M.N., Nucl. Fusion 18, 47 (1978).

7. Cohen, R.H., Rensink, M.N., Cutler, T.A. and Mirin, A.A., Nucl. Fusion 18, 122 (1978).

8. Catto, P.J., Bernstein, Ira B., Phys. Fluids 24, 1900 (1981).

9. LoDestro, L.L., "Steady-State Ion Distributions in a Potential and Magnetic Well," in Mirror Fusion Quarterly (April-June 1980); M.E. Harrison, E. O'Neal, (Eds.), Lawrence Livermore National Laboratory, Livermore, CA, UCRL-10060-80-2 (1980).

10. Carlson, G.A., et al., "Tandem Mirror Reactor with Thermal Barriers", UCRL-52836, 127 (1979).

11. Baldwin, D.E., "Barrier Physics", in Physics Basis for MFTF-B; Baldwin, D.E., Logan, B.G., and Simonen, T.C. (Eds.), Lawrence Livermore National Laboratory, Livermore, CA, UCID-18496-Part2, p. IV-92 (1980).

12. Rognlien, T.D., "Monte-Carlo Simulations of Tandem Mirror Physics", in Physics Basis for MFTF-B (UCID-18496-Part2) p. IV-179 (1980).

13. Li, Xing-Zhong, Emmert, G.A., University of Wisconsin Fusion Engineering Program Report UWFDM-393 (1980).

14. Li, Xing-Zhong, Emmert, G.A., University of Wisconsin Fusion Engineering Program Report UWFDM-419 (1981).

15. Li, Xing-Zhong, Emmert, G.A., Bulletin of the American Physical Society, 901 (1981).

16. Cohen, R.H., Nucl. Fusion 21, 209 (1981).

17. Pearlstein, L.D., Nevins, W.M., "The Barrier Potential Model", UCID-19159 (1981).

18. Carrera, R., Callen, J.D., University of Wisconsin Fusion Engineering Program Report UWFDM-466 (1982).

19. BenDaniel, D.J., Allis, W.P., Plasma Physics (Journal of Nuclear Energy Part C) 4, 31 (1961).

20. Li, Xing-Zhong, Emmert, G.A., University of Wisconsin Fusion Engineering Program Report UWFDM-490 (1982).

21. Li, Xing-Zhong, Emmert, G.A., University of Wisconsin Fusion Engineering Program Report UWFDM-524 (1983).

22. Sivukhin, D.V., "Coulomb Collisions in a Fully Ionized Plasma" in Reviews of Plasma Physics, edited by Acad. Leontovich M.A., Vol. 4, p. 93 (1966).

23. Hooper, E.B., private communication (1983).

24. Hildebrand, F.B., Introduction to Numerical Analysis, 2nd Edition (McGraw-Hill, 1974), p. 392.

25. Gradshteyn, I.S. and Ryzhik, I.W., Table of Integrals, Series, and Products (Academic Press, New York, 1965), p. 337.

ACKNOWLEDGMENT

Support for this work has been provided by the U.S. Department of Energy and the Wisconsin Electric Utilities Research Foundation (WEURF).